Evaluation of Accelerometer-Based Walking-Turn Features for Fall-Risk Assessment in Older Adults

by

Dylan John Drover

A thesis
presented to the University of Waterloo
in fulfillment of the
thesis requirement for the degree of
Master of Applied Science
in
Systems Design Engineering

Waterloo, Ontario, Canada, 2017

Author's Declaration

This thesis consists of material all of which I authored or co-authored: see Statement of Contributions included in the thesis. This is a true copy of the thesis, including any required final revisions, as accepted by my examiners. I understand that my thesis may be made electronically available to the public.

Statement of Contributions

Dr. Jonathan Kofman and Dr. Edward Lemaire, as Dylan Drover's supervisors, assisted with project conceptualization, and creation of the data collection and analysis protocols. Dr. Jennifer Howcroft assisted in project conceptualization, as well as developed and performed the data collection described in Section 3.1 in this thesis.

Dr. Jonathan Kofman, Dr. Edward Lemaire and Dr. Jennifer Howcroft also participated in editing and writing manuscripts submitted to and prepared for submission to peer reviewed journals that served as the basis for Chapters 4, 5 and 6. Dylan Drover was the major contributor and first author on both manuscripts. First drafts were written by Dylan Drover, and he was involved in every stage of editing. Dr. Jonathan Kofman and Dr. Edward Lemaire participated in editing all thesis chapters.

Abstract

Falls in older adult populations are a serious health concern, resulting in physical and psychological trauma in addition to increased pressure on healthcare systems. Faller classification and fall risk assessment in elderly populations can facilitate preventative care before a fall occurs. Few research studies in the fall risk assessment field have focused on wearable-sensor-based features obtained during walking-turns. Examining turn based features may improve fall-risk assessment techniques.

Seventy-six older individuals (74.15 ± 7.0 years), categorized as prospective fallers (28 participants) and non-fallers (43 participants), completed a six-minute walk test with accelerometers attached to their lower legs and pelvis. Turn and straight walking sections were segmented from the six-minute walk test, with a feature set extracted for each participant.

This work aimed to determine if significant differences between prospective faller (PF) and non-faller (NF) groups existed for turn or straight walking features. A mixed-design ANOVA with post-hoc analysis showed no significant differences between faller groups for straight-walking features, while five turn based features had significant differences (p <0.05). These five turn based features were minimum of anterior-posterior REOH for right shank, SD of SD anterior left shank acceleration, SD of mean anterior left shank acceleration, maximum of medial-lateral FQFFT for lower back, and SD of maximum anterior left shank acceleration. Turn based features merit further investigation for distinguishing PF and NF.

A novel prospective faller classification method was developed using accelerometer-based features from turns and straight walking. Cross validation was conducted for both turn and straight feature based models to assess classification performance. The best "classifier model – feature selector" combination used turn data, random forest classifier, and select-5-best feature selector (73.4% accuracy, 60.5% sensitivity, 82.0% specificity, 0.44 Matthew's Correlation Coefficient (MCC)). Using only the most frequently occurring features, a feature subset achieved better classification results, with 77.3% accuracy, 66.1% sensitivity, 84.7% specificity, and 0.52 MCC score (minimum of anterior-posterior ratio of even/odd harmonics for right shank, standard deviation (SD) of anterior left shank acceleration SD, SD of mean anterior left shank acceleration, maximum of medial-lateral first quartile of Fourier transform (FQFFT) for lower

back, maximum of anterior-posterior FQFFT for lower back). All classification performance metrics improved when turn data was used for faller classification, compared to straight walking data.

Acknowledgements

Special thanks to my supervisors, Dr. Jonathan Kofman and Dr. Edward Lemaire for their guidance, support and patience which have made this work possible. I would also like to thank Dr. Jennifer Howcroft for her advice and assistance throughout my MASc and my friends for their encouragement and companionship. Finally, I would like to thank my wonderful parents, Maribeth MacIntyre and Brad Drover, for their endless support throughout my life.

Table of Contents

List of Figures

List of Tables

List of Abbreviations

5FCV: Five-Fold Cross Validation

6MWT: Six-Minute Walk Test

ACC: Accuracy

ADS: Accelerometer Descriptive Statistic

ANOVA: Analysis of Variance

Ant: Anterior direction

CI: Confidence Interval

CM-FS: Classification Model-Feature Selector

CV: Cross Validation

FQFFT: First Quartile Fast Fourier Transform

Inf: Inferior direction

LB: Lower Back

LS: Left Shank

M: Subset of total number of data samples

MCC: Matthew's Correlation Coefficient

MFO: Most Frequently Occurring

MLE: Maximum Lyapunov Exponent

N: Total number of data samples

NF: Non-Faller

NPV: Negative Predictive Value

PF: Prospective Faller

Post: Posterior direction

PPV: Positive Predictive Value

REOH: Ratio of Even to Odd Harmonics

RF: Random Forest

RFE: Recursive Feature Elimination feature selector

RS: Right Shank

RSS: Random Shuffle Split

S5B: Select-5-Best feature selector

SD: Standard Deviation

SEL: Combined SFPR and SFDR feature selectors

SENS: Sensitivity

SFDR: Select False Discovery Rate

SFPR: Select False Positive Rate

S*k*B: Select-*k*-Best feature selector

SPEC: Specificity

ST: Stride-time

Sup: Superior direction

SVM: Support Vector Machine

TLE: Turn Location Estimation

TLI: Turn Limit Identification

TUG: Timed Up and Go

$\vec{w}$: Weight matrix

x: Data sample

***x*,** $\vec{x}$: Feature vector

y: Class label

Chapter 1
Introduction

Falls within elderly populations are a growing public health concern, with fatal and non-fatal fall injuries costing an estimated $23.3 billion in the United States, with a projected cost of $52 billion by 2020 [1,2]. Early fall risk detection and subsequent treatment are needed to mitigate fall incidence and improve quality of life for elderly individuals [3–5]. Wearable sensors that can be easily applied at the point-of-care [6–8] can facilitate quantitative assessments in clinical or older-adult care environments. Reviews of inertial-sensor applications for fall-risk classification in older-adults have recommended further research to determine if wearable sensors can be used to improve fall-risk prediction as a stand-alone assessment tool or supplement to clinical tests [8,9]. Combining appropriate wearable-sensor based features with machine learning techniques could advance fall-risk prediction tools and ultimately improve services for elderly people at risk of falling [7,10,11].

Fall risk prediction using clinical tests and wearable sensors has had variable success, with accuracy between 62 and 100%, specificity between 35 and 100%, and sensitivity between 55 and 99% [8]. While the top results are encouraging, some of the methods used retrospective faller populations or small samples sizes, or did not validate results by cross-validation, which suggests the need for further research. The lower performance rates indicate a need for alternative methods to achieve consistently high outcomes. Fall risk assessment research has primarily focused on clinical tests, composed mainly of straight level walking, multiple tasks (e.g., sit-stand, walk-turn), and balance challenging tasks (e.g., stand on one leg, reach). Few quantitative studies involve more than straight walking, such as turns, to predict fall risk [12]. This research evaluated accelerometer-based walking-turn features for fall-risk assessment in older adults. The evaluation compared turn and walking based features for prospective faller (PF) and non-faller (NF) groups, and developed wearable-sensor based faller-prediction models using straight-walking and walking-turn accelerometer-based features.

1.1 Rationale

Several studies have noted that turns can challenge stability maintenance and increase energy expenditure [13–16], and that turning time, steps per turn, and variability in the number

of steps across different turns are useful features for distinguishing fallers from non-fallers [12]. Subtle fall-risk related gait-based measures may become highly effective fall-risk indicators when applied to turns due to the increased challenge to stability, compared to straight walking. Individuals at high risk of falling employ different turning methods than healthy individuals [12,14], suggesting a distinction between fallers and non-fallers. A longer turn duration from the Timed Up and Go Test (TUG)[1] [17] discriminated elderly fallers from non-fallers. Clinical analysis of specific movements during turns, in combination with turn time and number of steps, discriminated between faller and non-faller groups [16]. Combinations of nine specific movements, turn time, and number of steps per turn also discriminated between multiple fallers, non-multiple fallers, and able bodied individuals [18]. The sum of this evidence strongly suggests that turns have gait-challenging characteristics and relevant features that distinguish between fallers and non-fallers. However, this research is limited by using few features and not incorporating wearable-sensor-based features.

Research that classifies fallers and non-fallers using multiple-site accelerometer-based features, for turning and straight walking, is lacking. Research is needed since accelerometers are the most common wearable sensors for movement assessment and quantitative differences between turn and straight walking features have yet to be determined. An extensive comparison of the same features for turn and straight walking may reveal suitable fall-risk indicators in either walking mode, which could aid future work in fall risk assessment. Existing literature supports the hypothesis that turn data may contain information that can discriminate between fallers and non-fallers better than straight walking data. However, previous research using turns has focused on clinical assessment tools, temporal variables (completion time), or video analysis for fall risk prediction [18–21]. Furthermore, a comparison between straight and turn walking features in faller classification models has not been reported. Such a comparison would be also useful in developing a better fall-risk assessment tool. Acceleration data acquired during the Six-Minute Walk Test (6MWT) [22] could provide both turn and straight walking information suitable for

[1] Timed Up and Go Test (TUG) is a fall-risk assessment test, where a participant begins seated in a chair, proceeds to stand up, then walks at a normal pace to a marker three metres away from the front of the chair, then turns around at the line (180 degrees), walks at a normal pace back towards the chair and sits back in the chair.

such an investigation. The hypothesis that this work aims to confirm is that turn-walking based accelerometer features will provide better discriminating ability between prospective fallers and non-fallers, and thus provide better faller classification performance than corresponding straight-walking based features. The objectives in the following section detail the procedures to assess this hypothesis.

1.2 Objectives

The objectives of this thesis research were:

1. Segment turn and straight walking sections from acceleration data (collected in a separate study during a 6MWT performed by older adults) and extract features.
    a. Develop a turn segmentation algorithm that identifies, from acceleration data, when a participant begins and ends a turning section. Straight sections are considered to be the non-turn sections of the data.
    b. From all turn and straight walking sections, extract accelerometer-based features (developed in previous work [7,23]) and create a new summary feature set over all sections, for each participant.
2. Perform statistical analysis on accelerometer-based features from turn-walking and straight-walking sections of the 6MWT performed by older adults.
    a. Determine which features differ significantly between the faller and non-faller groups, with turn and straight walking conditions treated separately.
    b. Determine which features differ significantly between turn and straight walking conditions, with fallers and non-faller groups treated separately.
    c. Determine if accelerometer-based features for turn data are superior to straight walking data for discriminating between fallers and non-fallers.
3. Develop and compare faller prediction models using walking-turn and straight-walking accelerometer-based features.
    a. Perform feature selection to determine the most appropriate features from 1(b), using both turn-walking and straight-walking data, and develop corresponding classification models for faller prediction.

b. Determine which feature subset from turn-based and straight-based data provide the best prediction results.
c. Assess if using turn-based features improves prediction results compared to straight-walking features.

1.3 Contributions

This research presents a statistical comparison between accelerometer-based features from prospective faller and non-faller groups, with straight and turn walking sections treated separately, to identify the subset of features that are significantly different, allowing for discriminating between the faller and non-faller groups. The statistical analysis also showed that accelerometer-based features for turns are more effective than the same features for straight walking in distinguishing fallers from non-fallers, and thus indicating fall risk. These results provide insight into the viability of turn acceleration data for fall risk assessment and identified features that are most effective in developing fall-risk assessment tools.

This research also presented novel wearable-sensor based faller classification models, using walking-turn and straight-walking accelerometer-based features, and compared classification metrics from these models to determine that turn acceleration data provides better results than straight walking data for prospective faller prediction. The research also determined which features provide the best classification (prediction) results.

Chapter 2
Background and Literature Review

2.1 Falls in Older Adults

Health care systems are under ever increasing pressure due to aging populations [24–26] with the annual healthcare cost of fall related injuries expected to reach $52 billion dollars by 2020 [2]. Falls constitute the leading cause of physical injuries in older adults [27] with consequences potentially leading to death [28]. Considerable social and personal ramifications for older adults are caused by falls; including, reduced mobility and activity [5,29–31], and decreased self-confidence and social interactions that may lead to depression [5,32]. These problem are compounded by de-incentivising desirable activities [3,4,32,33] that could help prevent future falls. The elderly falling issue is critical considering that 28 to 35% of people over the age of 65 will fall at some point [34,35], with the probability of falling increasing with age [36].

A large percentage of falls could be prevented if fall risk were predicted early and appropriate interventions taken [3,4,32,33]. Identification of risk factors or features to accurately predict or classify whether an individual is likely to fall in the future could permit early intervention to prevent a first fall. Current fall-risk assessment models have had variable results, suggesting a need for alternative fall-risk assessment methods [8,37].

2.2 Fall Risk Assessment

The literature has suggested that further research is required to determine if wearable sensors such as accelerometers might be appropriate tools for fall risk assessment [8,9,38]. Accelerometers have desirable qualities; such as, they can be easily worn, are non-invasive, and provide quantitative data that can relate to gait stability, either during a predetermined walking task or through activities of daily living [16]. A widely used test that incorporates a turn, but does not specifically focus on the turn information, is the Timed Up and Go (TUG) test [39]. TUG begins with a participant sitting in a regular arm chair, then the person stands up, walks at a normal pace to a line placed three metres from the front of the chair, turns around at the line (180 degrees), walks at a normal pace back towards the chair, and sits back in the chair. While popular

[8], TUG was suggested to not have general diagnostic accuracy for fall risk assessment due to widely varying thresholds for fall risk indicators between studies [37]. Varying performance metrics in fall risk assessment studies [8], possibly due, in part, to varying fall risk assessment validation methodologies [40], suggest that further work is needed to both explore new features for fall risk assessment but also modes of locomotion that have not been analyzed extensively, such as walking turns.

2.3 Turn Relevance

In a monitoring study, it was found that turn steps comprise between 8% to 50% of steps during various activities [16]. However, most studies focus on straight walking for gait analysis, leaving out a major part of human locomotion. One study found that a surveyed retrospective[2] repeated faller group had significantly slower mean peak turn speeds, longer mean turn durations, and more steps per turn than a non-faller group ($p < 0.05$) [12], and a prospective faller group had a significantly larger coefficient of variation for number of steps per turn than a non-faller group. Increased turn time and more steps during turning has been related to recurrent fall groups and difficulty while turning [20,21,41]. To assess local dynamic stability, which has been linked to fall risk [13], the maximum Lyapunov exponent (MLE) is often used. In able bodied participants, the MLE was greater for continuous, constant speed walking turning around a one metre radius circle, than for constant speed straight line walking, for hip, right knee and ankle locations [13]. These higher MLE values may indicate local instability while turning compared to straight line walking. Energy expenditure, measured as heartbeats per minute, was higher while performing 180 degree turns when compared to 90 degree turns [15]. A number of proposed clinical assessments for fall risk also included turns [18,19,42]. Aside from specific features that may distinguish fallers from non-fallers, elderly individuals used spin-turns (turns in which an individual pivots on one foot, using a spin to change direction) more frequently than step-turns (turns in which direction is changed by taking multiple steps to rotate the body), and

[2] Retrospective faller groups refer to surveyed participants who reported a fall within some timeframe (e.g., 6 or 12 months) prior to the fall-risk assessment test or experiment.

individuals at high risk of falling performed spin-turns more frequently than a low risk group [42,43].

Turn-based models for fall-risk assessment primarily used clinical assessments performed by a clinician or evaluation of primarily raw or immediately measurable features, such as number of steps per turn, heart rate, or turn timing. This approach, while valuable, does not account for more descriptive and comprehensive features that may be calculated from wearable sensor data (e.g., those based on harmonics of motion and frequency domain, and acceleration in multiple directions). Exploration of such features for turn walking could potentially improve fall risk assessment.

2.4 Extracted Features

A review of 40 inertial-sensor based fall risk studies found the dominant Fast Fourier Transform peak parameters (from lower-back accelerometers) and the ratio of even to odd harmonic (REOH) magnitudes (from head, upper back and lower back accelerometers) to both be recurring significant ($p < 0.05$) features when used to assess fall risk [8]. These features were carried forward in further research demonstrating their effectiveness for faller classification [7]. The dominant acceleration FFT peak parameter was adapted to the first quartile Fast Fourier Transform (FQFFT), composed of FFT coefficients below a frequency of 12.5 Hz. A lower FQFFT value would suggest the occurrence of a higher number of high frequency acceleration components while walking, which has been linked to instability [7,11,44]. Similarly, lower REOH values are associated with fall risk [45–49].

As noted in Section 2.3, variation between steps and general gait variability has been associated with fall risk [12,50], therefore the standard deviation of repeated measurements of features across a test may be useful for faller classification. Extreme values of features (maxima or minima) have provided more useful information than mean values [51], therefore maxima and minima should calculated for features whose values are repeated across a test.

2.5 Feature Selection

In the context of statistical classification, the input information to be classified is often formulated as "feature vectors" that are a set of numbers, categories, or other useful descriptors to represent the data. A feature vector forms a *d*-dimensional representation of the data, with each feature in the vector $\boldsymbol{x}$, representing a dimension, $x_i \ldots x_p$. These vectors can be thought of as *d*-dimensional points in the *d*-dimensional "feature space". A statistical classification model is defined by its parameters, θ. In some cases, there are more features (or dimensions, *d*) than the number of data samples, *N*, used for training a classifier model (i.e., $d >> N$). The number of model parameters is generally greater than or equal to the input dimension. If $d >> N$, insufficient information is available in the *N* data samples to optimize the large number of model parameters [52].

Classification difficulty arises if many features are non-informative (noise) or redundant (provide no new information). These features can lead to poor model generalizability since the model may be modelling noise in the features, leading to poor classification results [52]. One solution is to choose a subset of features that are non-redundant and informative for classification. This process is known as feature selection, which changes the case where $d >> N$ to the case where $N > d$. Practical and interpretability reasons exist for feature selection. Fewer dimensions can shorten model training time and simplify classification model performance analysis. For example, examining a feature vector with three features ($d = 3$) could provide more intuitive insight than a vector with 100 features ($d = 100$). A canonical example of high dimensional data would be a pixel based image, since each pixel is considered to be a dimension with a range of possible values. When dealing with motion data from accelerometers and gyroscopes on the legs, lower back, arms, and head, each axis generates information, which would lead to 36 features (6 body parts x 3 axes x 2 sensors) even before deriving how these feature values change across time or calculating and deriving further features.

The F-statistic feature selection method is based on F-statistics from a one-way analysis of variance (ANOVA) [53,54] and measures differences between feature means, depending on their given classification (group treatment). The features can then be ranked by their F-statistic

score. A subset with the highest scores are features with the greatest differences between means, accounting for variability within their own classes. As Equation 2.1 shows, the F-statistic can be interpreted as the ratio of inter-class and intra-class variabilities. A higher value corresponds to better separability between classes, because there is less class distribution overlap. A high F-statistic indicates proportionally more between-class variability than within-class variability.

$$F = \frac{\sum_{i=1}^{K} \frac{n_i(\bar{x}_i - \bar{x})^2}{(K-1)}}{\sum_{i=1}^{K}\sum_{j=1}^{n_i} \frac{\left(\bar{x}_{ij} - \bar{x}_i\right)^2}{(N-K)}} = \frac{between - class\ variability}{within - class\ variability}, \quad (2.1)$$

where n_i is the number of data points for the i^{th} class, $\bar{x}_i$ is the sample mean of the i^{th} class, $\bar{x}$ is the sample mean of all classes, *K* is the number of classes, *N* is the total number of examples and $\bar{x}_{ij}$ is the j^{th} example from the i^{th} class.

Recursive Feature Elimination uses a recursive process for feature selection [55,56]. A classifier that assigns weights to features (such as logistic regression) is chosen to perform classification on all features. After each iteration, a subset of the least weighted (weakest contributing) features is eliminated and the process is repeated until the desired final number of features is obtained.

2.6 Machine Learning Classifiers

Statistical classification models learn or define a function that translates input data (feature vectors) to output labels (classes). The data, represented as feature vectors, exist in a high dimensional "feature space", with each feature corresponding to a dimension. From the training set of feature vectors, a held-out testing set of feature vectors is used to determine if the model learned generalised parameters that can classify unseen examples. The "no-free-lunch" theorem [57] roughly states that no one model works best for every problem or data set; therefore, multiple types of classifiers should be tested and their performance evaluated to determine which best suit the data. The following sections briefly describe classifier models that were chosen for this research.

2.6.1 Support Vector Machine (SVM)

A support vector machine (SVM) is a linear classifier that attempts to create a decision boundary between two classes with the maximum-margin between the classes and the decision boundary [58]. This max-margin limits the chances of misclassification, assuming data points from similar classes will be close to their counterparts in the feature space. The decision boundary learned by a SVM is a plane or hyperplane, for feature space dimensions greater than 3, of the form:

$$\vec{w} \cdot \vec{x} - w_0 = 0, \tag{2.2}$$

$$\vec{w} \cdot \vec{x} - w_0 \geq 1, y_i = 1 \tag{2.3}$$

$$\vec{w} \cdot \vec{x} - w_0 \leq -1, y_i = -1 \tag{2.4}$$

where $\vec{x}$ is a feature vector, $\vec{w}$ are the coefficients that define the hyperplane in feature space, w_0 is the term that defines the maximum margin between data points of a class and the hyperplane. Class labels, y_i, have a value relative to the hyperplane of +1 or -1. The SVM optimization goal is to find the appropriate coefficients $\vec{w}$ and w_0 that maximize the distance (maximum margin) between the decision boundary and training examples.

If given classes are not linearly separable in the original feature space, SVMs can employ the "kernel trick" that creates a data projection into a higher dimensional space where a linear decision boundary may exist. A linear and polynomial kernel function were used in this research (Equation 2.5) to transform the given features and test for linear separation of the classes. The linear kernel is the case of the polynomial kernel, where d =1.

$$K(x, x') = (x^T x' + c)^d \tag{2.5}$$

where *d* and *c* are constants that can be adjusted to improve performance, *x* and *x'* are feature vectors. The kernel function *K* creates the mappings that make up the additional dimensions, where a new decision boundary is fit to the data [59].

2.6.2 K-Nearest Neighbours

K-nearest neighbours (*k*NN) is a non-parametric classifier that classifies an example (feature vector) based on the labels of its *k*-nearest neighbours in the feature space. Proximity or

"nearness" is chosen based on a distance metric (e.g., cosine distance, Euclidean distance). For a simple binary classification problem with class labels of -1 and +1, the class label of a given example *x* can be expressed as:

$$\hat{Y}(x) = \frac{1}{k} \sum_{x_i \in N_{k(x)}} y_i \tag{2.6}$$

where the neighbourhood $N_k(x)$ of *x* is defined by the *k* closest points x_i in the training data that have the labels y_i [52]. The average class of the area is the new label for testing example *x*. If *k* = 1, the decision boundary between classes will be very myopic and generally unsmooth, whereas larger *k* values will create a larger neighbourhood, creating class labels that are based on averages of more training samples. The single degree of freedom of the *k*NN makes it attractive for parameter searching. An alternative view of *k*NN classification is to estimate the probability that *x* belongs to a specific class, $p_c(x)$:

$$\widehat{p_c}(x) = \frac{M_c}{N \cdot |R(x)|} \tag{2.7}$$

where M_c are the points labelled for class *c* from the total number of desired observation points *M* from the training set, and $|R(x)|$ is a region that is expanded in the feature space until it contains the desired *M* samples [60].

2.6.3 Decision Trees and Random Forest

The Random Forest classifier uses the consensus of several decision trees to improve classification [61] by randomly sampling specific features and training examples from the data and fitting decision trees based on these subsets. The consensus of these trees provides better classification results than single decision tree classification [62]. Decision trees follow the terminology for data structure trees found in computer science. Decision trees consist of parent nodes (nodes with "child" nodes beneath them) that perform decisions based on rules and leaf nodes (nodes with no "child" nodes beneath them) which determine a class for data. The decision rules for parent nodes are in the form of:

$$f_m(\boldsymbol{x}): x_j > T_{m0} \tag{2.8}$$

where x_j is a specific feature of the feature vector $\boldsymbol{x}$ and T_{m0} is the threshold of the first node at the m^{th} level of the decision tree. The outcome of the decision determines which node will be evaluated next in the decision tree, or if the tree terminates in a leaf, (i.e., a classification) [61]. A simple example of a decision tree structure is shown in Figure 2.1.

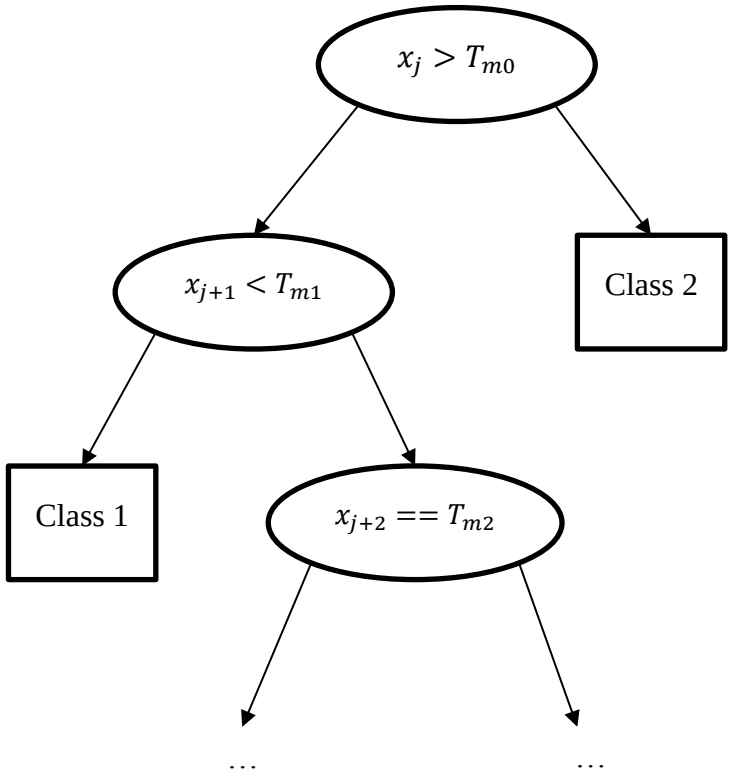

Figure 2.1. Simple example of decision tree structure (round nodes are parent (decision) nodes, square nodes are leaf (classifier) nodes).

The decision rules for nodes in a classification decision tree can be optimized using an *impurity measure*. A split is considered completely pure if, after the split, all classified training examples are from the same class. For a node *m*, the probability that a training example belongs to a class C_i is expressed as:

$$\hat{P}(C_i|\boldsymbol{x}, m) = \frac{N_m^i}{N_m} \tag{2.9}$$

where N_m^i is the number of training examples that belong to class C_i, and N_m is the total number of training examples.

2.7 Summary

The need for improved fall-risk assessment tools is apparent, with economic, social, and personal detriments for those affected by falls. Existing work has provided a foundation for wearable-sensor based assessment tools with some good results; however, potentially useful data sources (i.e., walking turns) and the use of turn-based specific features for fall prediction is still not adequately explored. The existing research suggests that both turn data and specific turn-based features may provide useful information for fall-risk assessment. These topics are explored and discussed in the following chapters.

Feature selection, though not specifically the methods detailed in Section 2.5, has been used in previous fall-risk assessment work. The machine learning classifiers detailed in Section 2.6 have been used in the fall-risk assessment literature [8]. Using these powerful tools in tandem, the following chapters provide analysis to assess the validity of the hypothesis proposed in Section 1.1.

Chapter 3
Data Collection and Processing

This first section of this chapter details the data acquisition protocol that was developed and performed by Dr. Jennifer Howcroft. Participants performed a controlled walking test that generated data used for the analyses described in Section 3.2 and Chapter 4 and 5. The second section of this chapter describes the methodology used to achieve Objective 1: Segment turn and straight walking sections from 6MWT and extract features. Data synchronization and the turn segmentation algorithm are described. Extracted features, a method of generating summary features for each participant, and normalization techniques are also detailed.

3.1 Data Collection

3.1.1 Participants

A convenience sample of 76 individuals, 65 years or older (mean 74.15 ± 7.0 years) was recruited from the community. Inclusion criteria were the ability to walk continuously and unaided for six minutes, no existing self-reported cognitive disorders, and not having experienced a fall during the six months prior to the study. Participants had a mean weight of 73.35 ± 13.4 kg and a mean height of 167.25 ± 10.0 cm. The study was approved by the University of Waterloo Research Ethics Committee. All participants gave informed written consent.

3.1.2 Protocol

Participants reported their age and sex. Accelerometers (X16-1C, Gulf Coast Data Concepts, Waveland, MS, USA) were fitted to the posterior pelvis (lower back, LB), left lateral shank (LS), and right lateral shank (RS) (Figure 3.1). Accelerometers were aligned with the vertical (upward: positive), medial-lateral (ML) (right: positive), and anterior-posterior (AP) axes (anterior: positive). Accelerometer data were collected at 50 Hz. The six-minute walk test (6MWT) was conducted under standard conditions. Participants walked along a hallway, making consecutive left and right turns around two cones spaced 30.34 m (100 ft) apart [22]. A six-month follow-up fall-occurrence survey identified participants who fell at least once as

prospective fallers (PF). All other participants were classified as non-fallers (NF). A fall was defined as an event that results in a person coming to rest unintentionally on the ground or other lower level, excluding falls from a stroke or overwhelming hazard [63].

Five participants were excluded because of accelerometer failure (two participants), unreliable data synchronization (one participant), incomplete prospective survey (one participant), and poor turn segmentation due to excessive noise between straight walking and turning sections (one participant). Therefore, 71 participants were included in the study, with 43 non-fallers and 28 prospective fallers.

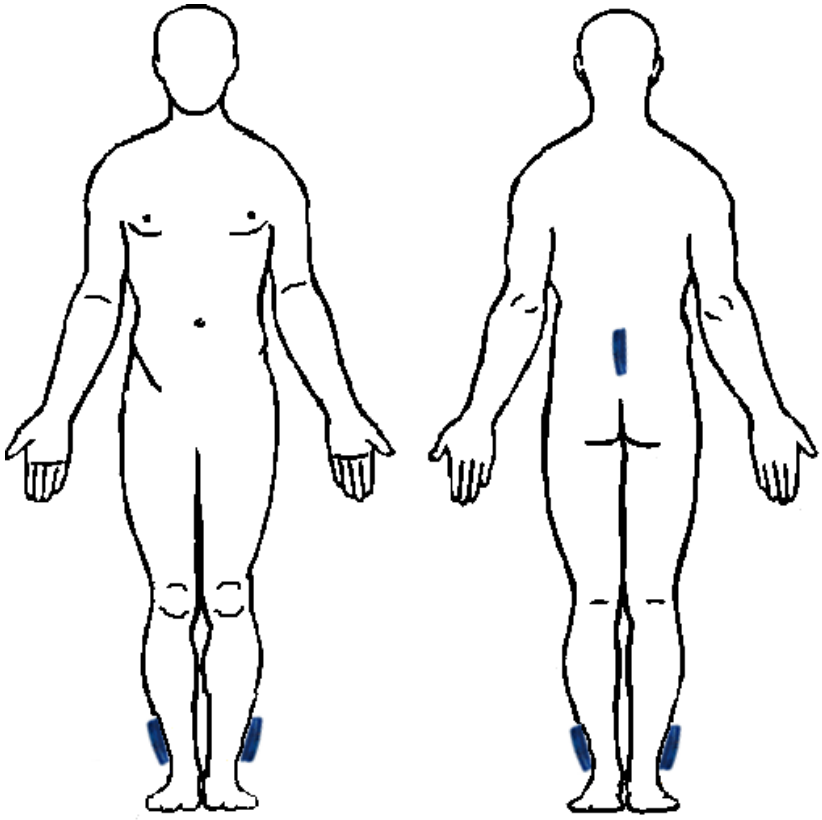

Figure 3.1. Accelerometer locations on participant, fitted to the posterior pelvis (lower back, LB), and left lateral shank (LS) and right lateral shank (RS).

3.2 Data Processing: Turn Segmentation and Feature Extraction

3.2.1 Accelerometer Signal Synchronization

Due to slightly differing sampling rates of the three accelerometers (lower back, left and right shanks), all data were first resampled to 50 Hz and then synchronized. MATLAB 2014b was used for all data processing [64]. The LB accelerometer had a vertical axis peak for each step, whereas LS and RS accelerometers only had vertical axis peaks for their respective steps. For each participant dataset, accelerometer signal synchronization was performed by manually aligning one shank and LB accelerometer signals using the first vertical peak or a reference spike. The other shank accelerometer and remaining LB signal peaks were then aligned. The peaks of the two shank accelerometers alternated at regular intervals. An example of synchronized RS and LS vertical accelerometer signals can be seen in Figure 3.2.

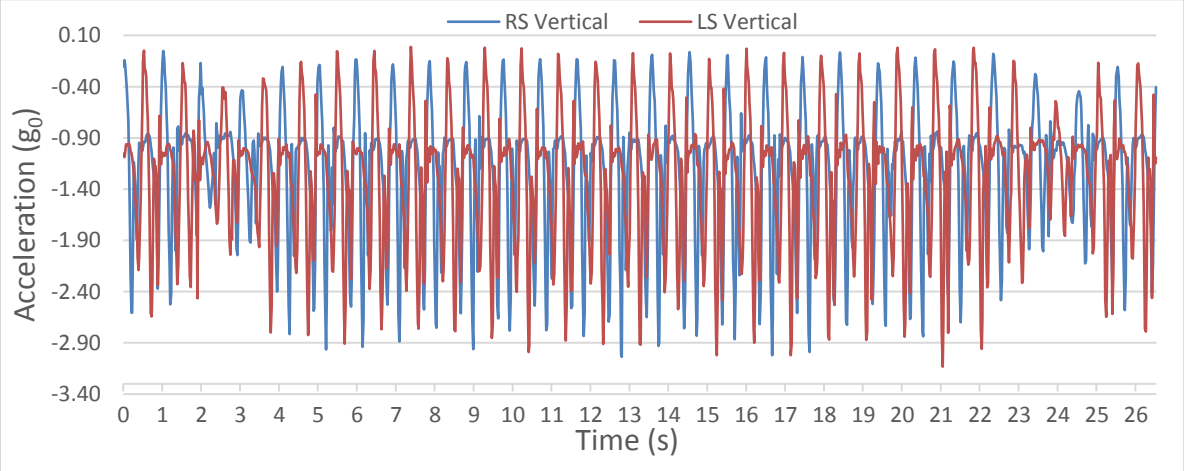

Figure 3.2. Synchronized RS and LS vertical accelerometer data.

3.2.2 Turn Segmentation

Accelerometer data for each participant were segmented into straight and turn sections. For the purposes of this research, a turn was standardized as having five steps: a centre step and two adjacent steps on each side of the centre step, plus a 0.2 seconds buffer before and after the first and last steps. Turn segmentation was performed using a two-stage process. The first stage, hereafter referred to as “turn location estimation” (TLE), estimated turn locations across the

6MWT data for each accelerometer signal using their vertical axis signal. The beginning of a step was defined as the beginning of a foot-fall, which corresponded with vertical acceleration peaks. The second stage, referred to as "turn limit identification" (TLI), examined all estimated TLE locations to identify the specific five steps that were defined as the limits of a turn.

TLE began by identifying a decrease, and corresponding increase, in amplitude of vertical component peaks for all three accelerometers [14] (Figures 3.2 and 3.3). A fifth order Butterworth low-pass filter with a cut-off frequency of 2.5 Hz was applied to all vertical accelerometer signals to attenuate noise before detecting peaks. A spline was fitted to the peaks of each filtered vertical accelerometer signal. The vertical value of this spline remained relatively constant (i.e., slope of the spline was roughly horizontal) during straight walking but decreased in magnitude during turns, corresponding to the decrease in the amplitude of peaks during turns. The locations of the relative minima for each acceleration spline was an estimated turn location. If at least two acceleration splines had estimated turn locations within a period of 1 s, the values of the estimated turn locations were averaged as the final TLE and would subsequently be a region searched by the TLI in the next turn segmentation stage. This generated a series of estimated turn locations for each participant.

TLI was performed to segment all turns generated by the TLE stage. Turns had a common pattern of characteristics that permitted segmentation. By superimposing the RS and LS vertical acceleration signals (Figures 3.2 and 3.3), a central footstep in the turn (from either the right or left foot) would have the smallest amplitude vertical peak acceleration. From this starting point, two adjacent footsteps on either side of the centre footstep composed the turn limits.

The turn's footstep identification procedure was:

1. Examine ±1.5 second window centred on the i^{th} TLE location (TLE_i).
2. Perform peak detection for the vertical LS and RS acceleration signals.
3. Create a combined time ordered list of detected peaks (t, p) from Step 2 (LS and RS signals, e.g., $(t_1, p_1)_{LS}$, $(t_2, p_2)_{RS}$ … $(t_n, p_n)_{LS}$).
4. Find smallest amplitude peak (centre footstep) and the two adjacent footsteps (peaks) before and after centre footstep from the ordered list in the Step 3.

5. Add a buffer before and after the first and last footsteps, respectively, with ±10 data points (0.2 s) and store these limits as a segmented turn.
6. Repeat the above procedure for TLE_{i+1}, if there exists a TLE_{i+1}.

The dynamically generated start and end permits turn sections to have different durations throughout the numerous 6MWT turn sections. The turn segmentation algorithm was run for each participant and visually inspected after completion. Errors in segmentation were corrected manually if automatic segmentation failed. Straight sections were defined as non-turn sections, where a participant completed walking the full 30.32 m (100 ft) path between cones. This created a 1:1 ratio between the number of straight and turn sections.

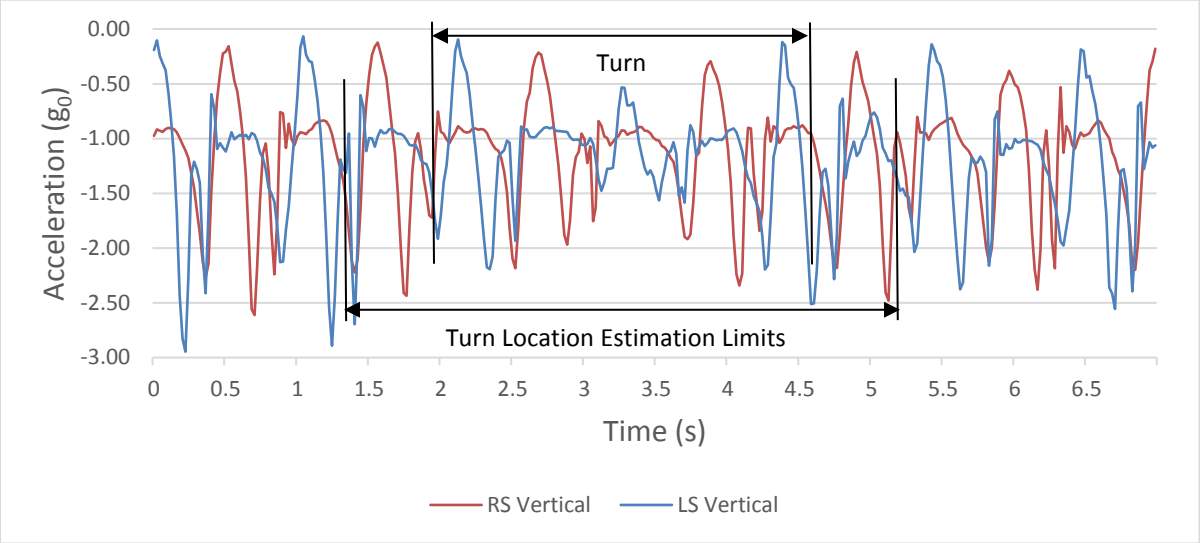

Figure 3.3. Vertical acceleration from right shank (RS) and left shank (LS) with general turn region and final segmented turn section.

3.2.3 Feature Extraction

The following accelerometer-based features were calculated for each stride and then averaged across all strides, for each turn or straight section:

- Temporal: Cadence, stride time.
- Acceleration descriptive statistics: Acceleration maximum, mean, standard deviation for each direction for each of three axes (positive and negative of vertical, ML, and AP axes).

- Acceleration frequency: First quartile of Fourier transform (FQFFT) of each axis (i.e., frequencies below 12.5Hz).
- Ratio of even/odd harmonics (REOH): Ratio of acceleration signal in phase with stride frequency [47,48,65].

Twenty-four features were extracted for accelerometers: three descriptive statistics for each of three axes in both the positive and negative directions (3x3x2=18 features), FQFFT for three axes, and REOH for three axes. Cadence and stride time were calculated from acceleration measured by the lower-back accelerometer, for a total of 26 features for the lower back. Each straight and turn section had a total of 74 features (24 for left and right shanks, 26 for lower back: 24+24+26 = 74 features).

The number of completed walk and turn sections differed between participants because of differing walking speeds over the six minutes of the test (i.e., a participant may have completed more laps (more straight and turn sections) than another participant who walked more slowly). Since participants with more feature sets could have a disproportionate effect on model training, a single feature set was created for each participant using the maximum, minimum, standard deviation, and mean of the 74 features across a participant's straight or turn sections. This produced a feature set with 4x74 = 296 features for each participant's turn or straight sections. This data treatment provided a number of potential benefits since extreme values (maximum and minimum) provide useful information for fall risk assessment [51] and variation in number of steps across turning sections was useful for distinguishing recurrent fallers and non-fallers [12]. The large number of features provided a starting point for exploratory feature analyses, which determined the best features for fall-risk assessment (explored in Chapter 4). For faster model training [66,67] each feature value in a participant's feature set was normalized to the range [0, 1] as follows:

$$y_{\text{normalized}} = \frac{y - y_{\min}}{y_{\max} - y_{\min}} \tag{3.1}$$

where y is a feature value from one participant, and y_{min} and y_{max} are the minimum and maximum values of that feature, respectively, across all participants.

3.3 Summary

The work detailed in this chapter focused on achieving the goals from Objective 1 from Section 1.2. A six-minute walk test was performed using three accelerometers for 74 participants. This data was resampled and synchronized to allow further processing. A turn segmentation algorithm was developed to segment both turning and straight-walking sections from the accelerometer data of each participant, satisfying Objective 1a. Features were extracted for each of these sections, with each participant having multiple sets of features for their trial. Statistics across sections for a participant were calculated, and one consolidated feature set, representing the entire participant trial, was generated for each participant. Feature extraction and consolidation achieved the goals outlined in Objective 1b. With the feature sets for both turn data and straight data computed, statistical analysis and generation and comparison of faller prediction models could then be undertaken, as detailed in the following chapters.

Chapter 4
Statistical Analysis of Turn and Straight Walking Accelerometer Features

The following section presents the outcomes for Objective 2: Perform statistical analysis on accelerometer-based features from turn-walking and straight-walking sections of the 6MWT performed by older adults. This chapter focuses on the statistical analysis and comparative analysis of turn walking and straight walking accelerometer-based features.

4.1 Statistical Analysis Methods

A mixed-design ANOVA test was performed for each feature, using faller status (faller or non-faller) for the two-factor between-subject variable and walking condition (straight or turning) for the two-factor within-subject variable ($p < 0.05$). From this ANOVA, features with significant differences ($p < 0.05$) for faller status, walking condition, or interaction effects were further analyzed in a post-hoc analysis. The first step of the post-hoc analysis was to determine whether a feature's distribution was normally distributed. This is important since different statistical tests should be performed for non-normally and normally distributed data. The Shapiro-Wilk test ($\alpha < 0.05$) [68] was used to assess normality of a feature's distribution, which would determine which test to use in the post-hoc analysis.

Turn and straight walking conditions were compared for each feature using paired *t*-tests for features with normal distributions and Wilcoxon Signed-Rank tests for features with non-normal distributions [69], with each test treating faller and non-faller data separately. Faller status (prospective faller or non-faller) was analysed for each feature with independent samples *t*-tests for normal distributions and Mann-Whitney U-tests [70] for non-normal distributions, with straight and turn features treated separately. A significant result from the faller status comparison tests would indicate that the feature could be used to discriminate between the two faller groups. To compensate for multiple comparisons, all *p*-values for post-hoc tests were corrected using the Benjamini-Hochberg (BH) method [71,72]. Using the BH method and a false discovery rate of 5%, significance for turn features required uncorrected *p*-values of $p < 0.00694$ and for straight walking features significance required uncorrected *p*-values of $p < 0.00139$. All data analysis was conducted using the R programming language [73].

4.2 Results

4.2.1 Post-Hoc Results for Faller Status Tests

No descriptive statistic features were found to be significantly different between PF and NF for straight walking (Table 4.1). However, for turns, three ADS features had significantly lower values for PF: standard deviation (SD) of the mean anterior acceleration for the left shank accelerometer was (0.049±0.03) for PF and (0.075±0.032) for NF, SD for SD of anterior left shank acceleration was 0.063±0.032 for PF and 0.091±0.031 for NF, and SD of the maximum anterior left shank acceleration was 0.241±0.116 for PF and 0.302±0.101 for NF.

For FQFFT and REOH features during turns (Table 4.2), PF had a significantly lower maximum FQFFT in the medial-lateral axis for the lower back accelerometer (75.92± 12.43) compared to NF (84±8.95). No FQFFT features were significantly different for straight section features. The minimum REOH of the anterior-posterior axis for right shank accelerometer was significantly greater for PF, for turning section features. No REOH features were significantly different for straight section features.

Table 4.1. Means, standard deviations, and *p*-values between faller and non-faller groups for turn and straight walking conditions for descriptive statistic features. Max: maximum, Min: minimum, SD: standard deviation, Post: posterior direction, Ant: anterior direction, RS: right shank, LS: left shank, LB: lower back, $\bar{x}$: mean. Bold indicates a significant difference ($p < 0.05$) after multiple test correction.

Feature	Turn					Straight				
	Fallers		Non-Fallers			Fallers		Non-Fallers		
	$\bar{x}$	SD	$\bar{x}$	SD	*p*	$\bar{x}$	SD	$\bar{x}$	SD	*p*
Max SD Post. RS	0.353	0.102	0.385	0.123	0.340	0.354	0.105	0.347	0.093	0.783
Max Mean Ant. RS	0.479	0.179	0.579	0.237	0.047	0.518	0.179	0.667	0.282	0.017
Max SD Ant. RS	0.545	0.223	0.657	0.237	0.024	0.579	0.168	0.740	0.288	0.004
Max Mean Ant. LS	0.412	0.201	0.514	0.208	0.017	0.535	0.207	0.644	0.228	0.033
Max Mean Ant. LB	0.243	0.131	0.315	0.172	0.101	0.218	0.104	0.277	0.120	0.018
Min Mean Post. RS	0.199	0.078	0.200	0.069	0.678	0.279	0.074	0.309	0.079	0.115
Min Mean Ant. RS	0.238	0.081	0.269	0.109	0.317	0.423	0.126	0.532	0.212	0.033
Min SD Ant RS	0.190	0.082	0.237	0.125	0.172	0.483	0.146	0.611	0.243	0.021
Min Max Ant. RS	0.752	0.269	0.899	0.413	0.072	1.706	0.488	2.006	0.697	0.119
Min Mean Ant. LS	0.248	0.115	0.258	0.118	0.653	0.444	0.159	0.528	0.193	0.069
Min SD Ant LS	0.238	0.121	0.248	0.125	0.695	0.512	0.184	0.586	0.189	0.106
Min SD Ant LB	0.123	0.074	0.158	0.116	0.396	0.138	0.062	0.176	0.078	0.021
Mean Mean Ant RS	0.348	0.123	0.410	0.163	0.141	0.464	0.136	0.596	0.248	0.021
Mean SD Ant RS	0.344	0.130	0.431	0.182	0.043	0.531	0.157	0.676	0.265	0.018
Mean Max Ant. RS	1.296	0.444	1.536	0.570	0.089	1.851	0.527	2.193	0.742	0.026
Mean Mean Ant. LB	0.181	0.087	0.227	0.118	0.187	0.192	0.090	0.239	0.103	0.021
Mean SD Ant LB	0.167	0.089	0.207	0.125	0.311	0.160	0.069	0.213	0.104	0.018
Mean Max Ant. LB	0.598	0.280	0.700	0.388	0.458	0.541	0.209	0.695	0.303	0.020
SD SD Ant RS	0.106	0.050	0.126	0.044	0.067	0.029	0.019	0.037	0.019	0.018
SD SD Right LS	0.047	0.017	0.057	0.021	0.062	0.015	0.008	0.017	0.009	0.212
SD Mean Post. LS	0.041	0.017	0.049	0.023	0.157	0.013	0.005	0.018	0.008	0.021
SD SD Post. LS	0.037	0.015	0.045	0.022	0.216	0.013	0.004	0.016	0.006	0.117
SD Max Post. LS	0.140	0.044	0.172	0.067	0.018	0.055	0.018	0.071	0.030	0.023
SD Mean Ant. LS	0.049	0.030	0.075	0.032	**p<0.001**	0.028	0.020	0.033	0.016	0.046
SD SD Ant LS	0.063	0.032	0.091	0.031	**p<0.001**	0.025	0.011	0.029	0.011	0.064
SD Max Ant. LS	0.241	0.116	0.302	0.101	**0.003**	0.070	0.026	0.084	0.031	0.111
SD Mean Inf. LB	0.023	0.013	0.029	0.016	0.111	0.011	0.008	0.015	0.008	0.007

Table 4.2. Means, standard deviations, and *p*-values between faller and non-faller groups for turn and straight walking conditions for first quartile of fast Fourier transform and ratio of even to odd harmonics features. Max: maximum, Min: minimum, SD: standard deviation, AP: anterior-posterior axis, ML: medial-lateral axis, V: inferior-superior/vertical axis, RS: right shank, LS: left shank, LB: lower back, $\bar{x}$: mean. Bold indicates a significant difference ($p < 0.05$) after multiple test correction.

Feature	Turn					Straight				
	Fallers		Non-Fallers			Fallers		Non-Fallers		
	$\bar{x}$	SD	$\bar{x}$	SD	*p*	$\bar{x}$	SD	$\bar{x}$	SD	*p*
Max FQFFT AP RS	71.06	13.35	78.05	11.52	0.175	14.38	6.68	15.60	8.59	0.409
Max FQFFT AP LS	69.73	12.94	77.03	9.65	0.027	16.34	7.35	17.07	8.90	0.619
Max FQFFT AP LB	75.51	10.50	81.63	6.73	0.021	14.35	8.46	14.25	7.55	0.670
Max FQFFT ML LB	75.92	12.43	84.00	8.95	**0.005**	12.09	5.91	13.94	8.68	0.450
SD FQFFT AP RS	7.24	4.62	9.60	4.31	0.057	1.82	1.58	1.88	1.82	0.757
SD FQFFT V RS	7.11	3.36	9.39	3.72	0.012	1.96	2.84	2.08	3.05	0.829
SD FQFFT ML LB	7.55	4.89	10.27	4.78	0.024	1.83	1.54	2.12	2.01	0.865
Min REOH AP RS	0.710	0.104	0.627	0.078	**0.001**	0.600	0.122	0.570	0.165	0.379
Mean REOH AP LB	1.147	0.207	1.263	0.293	0.056	2.645	0.704	3.066	0.995	0.041

4.2.2 Post-Hoc Results for Walking Condition Tests

With separate analyses for PF and NF groups, significant differences between turns and straight walking were found (Tables A.1 - A.7 in Appendix A). The initial ANOVA test produced 254 features for post-hoc analysis, which resulted in 231 features having significant differences between turn and straight walking for the faller group (91% of features). The non-faller group had 234 features with significant differences between turn and straight walking (92% of features).

Most features had significantly different means between turns and straight sets, for both faller and non-faller groups. Eleven of twenty non-significant features for NF were ADS means. This trend was less prevalent for PF, with only eight of 23 non-significant features as ADS means. Faller and non-faller groups had eight non-significant features in common, with 15 non-significant features unique to the faller group and 12 unique to the non-faller group.

4.3 Discussion

This research demonstrated the importance of measuring turn biomechanics as part of an elderly fall-risk assessment. Significant differences between PF and NF groups were found for

turning features; however, no significant between-groups differences were found for similar features from straight walking data. These results confirmed the hypothesis that turn data contains important information that can be used to establish differences between faller and non-faller groups, and that future fall-risk assessment research should consider turn-based features. This exploratory research also identified many relevant accelerometer features that differed between turning and straight walking conditions, for both prospective fallers and non-fallers, thereby providing a basis for developing accelerometer wearable-sensor based fall-risk models.

Data was generated from a common, standardized test (6MWT); therefore, the results from this work can be easily integrated into clinical and elderly care environments. Five turn-based features were significantly different between PF and NF groups, with lower values in the PF group for four of these measures. Lower variability measures across turn sections were effective in distinguishing between PF and NF (SD of the mean anterior left shank acceleration, SD of anterior left shank acceleration SD, SD of the maximum anterior left shank acceleration). The low variability in these SD features, which were all associated with the left shank anterior acceleration, likely indicates less variability in the non-dominant leg of most participants. Lower FQFFT for the lower back accelerometer's medial-lateral axis indicated that PF had higher frequency components in their gait. Walking characteristics composed of higher frequencies have been associated with fall risk [11]. The right shank accelerometer's minimum anterior-posterior REOH was greater for PF than NF. This result conflicts with previous research that suggests that individuals at risk of falling have a lower REOH [45–49]. Only one feature with a significant difference was based on the mean acceleration. This supports the suggestion that extreme values are more useful in differentiating between PF and NF [51].

Features that had statistically significant differences between faller groups could be used for fall risk classification, since these features likely allow the faller classes to be separated by a machine learning classifier. The post-hoc analysis determined that, for straight walking data, no features had a significant difference between PF and NF groups. This suggests that these features would not be viable for use in a fall risk classifier or fall risk assessment; however, the five turn data features with significant differences between PF and NF groups should be considered.

The comparison between turn and straight walking showed significant differences for some temporal features, which indicated a slower, more variable gait during turns for both PF and NF. SD for cadence and stride time were greater between turn sections than between straight sections, showing greater gait variability across turns in the 6MWT. More gait variability has been linked to fall risk [12,50].

All FQFFT features (Table A.6) had significantly greater values for turns compared to straight walking. These results are surprising since a lower FQFFT is associated with more high frequency components, which are linked to instability [7,11,44]. A lower FQFFT showing less stability was expected.

Chapter 5
Faller - Non-Faller Classification

This chapter details the methodology to achieve Objective 3: Develop and compare faller prediction models using walking-turn and straight-walking accelerometer-based features. Feature selection techniques, the selected features, cross validation methods developed, and performance evaluation of machine learning classifiers are described. Results from three experiments are detailed and discussed.

5.1 Feature Selection

Feature selection was performed to eliminate redundant and non-informative features before classification [53,54,67]. Three feature selection methods (feature selectors) were used for each respective classifier to assess performance. The first feature selector, Select-*k*-Best, selected features that accounted for the most variance between classes. The variable *k* was set to 5 based on a heuristic search (Select-5-best, S5B). The second feature selector (SEL) was based on Select False Positive Rate (SFPR) and Select False Discovery Rate (SFDR) methods, which chose features that minimized false positive and false discovery rates, respectively. The resulting list of SFPR and SFDR selected features were concatenated into a single non-redundant list. The number of features selected with SEL was not restricted. The third feature selector, recursive feature elimination (RFE), performed multiple data classifications using a random forest classifier, kept features that provided better classification results, and eliminated features with poorer results. This process was repeated until five best features were selected. Feature selection was performed only on training data for the classifier models. The selected features were then applied to the testing data for classification.

5.2 Classification

5.2.1 Machine Learning Models

Six classifier models were trained to classify participants as faller or non-faller: two *k*-nearest neighbor classifiers with k=3 (3NN) and k=5 (5NN); three support vector machines (SVM) with linear, third, and fifth order polynomial kernels; and one random forest (RF) model.

RF and *k*NN are non-parametric models that allow irregular class boundaries. All SVMs used a method where overlapping classes may become separable by using the "kernel trick" by projecting the data into higher dimensions [58,74]. RF is an ensemble method that creates a strong classifier based on many decision trees, thereby accommodating individual tree weaknesses. One hundred decision trees were trained for each RF classifier. Models were generated with the Scikit-Learn library [55].

5.2.2 Cross Validation

A subset of the full dataset was used for model training, and the remaining data subset was used to test model performance. Two cross validation (CV) methods were used: Five-fold cross validation (5FCV) and 2500-iteration random-shuffle-split cross validation (2500-RSS). Both methods used stratified data splits, which ensured that the ratio of fallers to non-fallers from the whole dataset was preserved in both the training and testing data.

5FCV divided the data into five stratified subsets (20% data in each subset), with one subset chosen for model testing and the remaining four subsets combined for model training. The three feature selectors (Select-*k*-Best, SEL and RFE) were applied to the training subset, thereby providing three best feature sets for classification. Classifier training (on four subsets combined) and testing (on the fifth subset) were then performed five times such that every subset was used as the testing set. The five sets of results were averaged to obtain final results for each classification-model – feature-selector (CM-FS) combination. With six classifier methods and three feature selection methods, a total of 18 CM-FS combinations were generated from 5FCV. The best CM-FS combinations were used in the 2500-RSS for both straight and turn-based data.

For 2500-RSS, a single stratified-random-shuffle split was configured to select a stratified random subset of 80% of the data for training the model with the remaining 20% of the data as a stratified random subset for model testing. This process was repeated for 2500 iterations. For each iteration, feature selection was performed on the training data and a new classification model was trained and tested. Feature selection was based solely on cross validation iteration training data. Mean, standard deviation, and confidence interval were calculated based on results from the 2500 iterations. Unlike 5FCV, this method does not

guarantee that all testing subsets will be disjoint. However, because of the large number of iterations, many unique data splits will determine if the models generalize well. The chosen number of iterations was based on convergence of the classifier mean accuracy.

5.2.3 Performance Evaluation

Performance for each CM-FS combination was evaluated using accuracy (ACC), specificity (SPEC), sensitivity (SENS), negative predictive value (NPV), positive predictive value (PPV), F1 score, and Matthews Correlation Coefficient (MCC) [75,76]. For 5FCV, means for these metrics were calculated over the five cross-validation folds. For 2500-RSS, mean, standard deviation and confidence interval of these metrics were calculated over the 2500 iterations. To determine the best performing CM-FS combination, classifier performance metrics were sorted in descending order with the largest result (best) given a value of 1, the second a 2, etc. Ties were given the same rank, with the next non-tied classifier being ranked by their position after accounting for the tied classifiers (e.g., a three-way tie at position three results in: 1, 2, 3, 3, 3, 6, 7, …) [77]. Rankings were summed across performance measures, with the lowest sum indicating the best classifier. This generated one score for each CM-FS combination.

Three tests were performed for both straight and turn data (Figure 5.1). Test I used 5FCV for all 18 CM-FS combinations (six classifiers, three feature selectors). The top-nine combinations were evaluated and one classifier and one feature selector that appeared the least were discarded, for both straight and turn results, which expedited training. The 10 remaining CM-FS combinations were used in Test II. Test II used 2500 RSS cross validation to evaluate performance of the remaining five classifiers and two feature selectors combinations (10 CM-FS combinations).

For Test III, the most frequently occurring (MFO) features from the feature selections of Test II, selected for 250 or more iterations (selected for 10% of the iterations from 2500-RSS CV), were combined into multiple sets. The entire set of most frequent features was ordered from most frequent (f_0) to least frequent (f_n), $X_0 = [f_0 \ldots f_n]$. The first set was composed of all the most frequent features, $X_0 = [f_0 \ldots f_n]$, the second set was composed of the n-1 most frequent features, $X_1 = [f_0 \ldots f_{n-1}]$, the third set was composed of the n-2 most frequent features,

$X_2 = [f_0 \ldots f_{n-2}]$, and so on until the final subset had only the most frequent feature $X_n = [f_0]$. Starting with a set of all the most frequent features to a final set having one feature, 2500-RSS cross validation was performed for each new generated feature set X_i, where $i = [0, n]$ (Figure 5.2), using the best classifier model from Test II. This analysis was performed for straight and turn data. Test III determined the best subsets of features for faller classification.

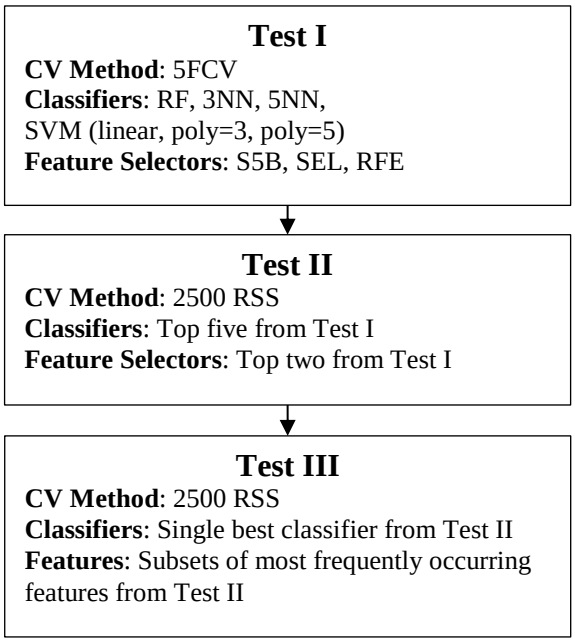

Figure 5.1. Model performance evaluation tests.

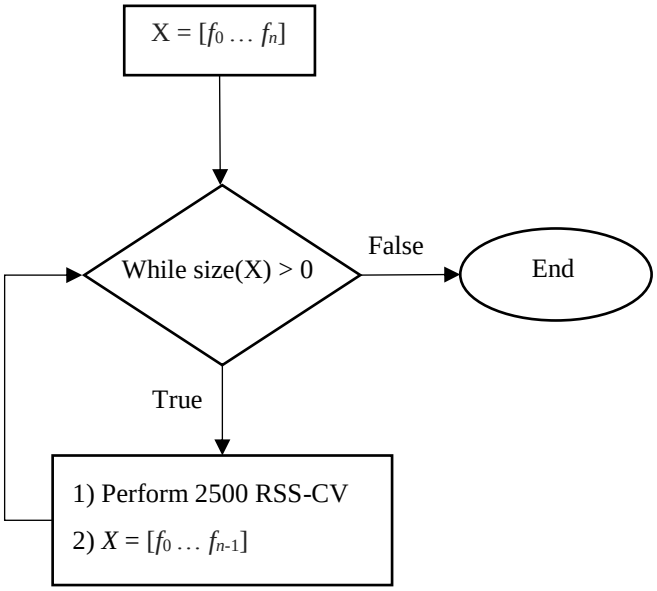

Figure 5.2. Test III procedure for testing most frequently occurring feature subsets.

5.3 Results

5.3.1 Test I

Test I results for straight-walking using 5FCV are presented in Table 5.1. The RF and S5B combination was the best with 62.0% accuracy, 46.4% sensitivity, 72.1% specificity and 0.19 MCC. The second-best model also used S5B feature selection, and had greater sensitivity (78.6%) but lower specificity and accuracy.

Table 5.1. Straight-walking section 5FCV results. PPV: positive predictive value, NPV: negative predictive value, MCC: Matthews correlation coefficient, S5B: select-5-best, SEL: false positive and discovery rate method, RFE: recursive feature eliminator, RF: random forest, *k*NN: *k*-nearest neighbour, SVM: support vector machine, linear: linear kernel, poly: polynomial kernel.

Classifier, Feature Selector	Accuracy (%)	Sensitivity (%)	Specificity (%)	PPV (%)	NPV (%)	F1 Score	MCC	Rank Sum
RF S5B	62.0	46.4	72.1	52.0	67.4	0.49	0.19	24
SVM (poly = 3) S5B	56.3	78.6	41.9	46.8	75.0	0.59	0.21	26
RF SEL	57.7	46.4	65.1	46.4	65.1	0.46	0.12	36
RF RFE	62.0	32.1	81.4	52.9	64.8	0.40	0.16	44
SVM (poly = 5) SEL	54.9	57.1	53.5	44.4	65.7	0.50	0.10	46
SVM (poly = 3) RFE	52.1	71.4	39.5	43.5	68.0	0.54	0.11	47
SVM (poly = 3) SEL	52.1	71.4	39.5	43.5	68.0	0.54	0.11	47
*k*NN *(k* = 5) SEL	56.3	42.9	65.1	44.4	63.6	0.44	0.08	51
*k*NN *(k* = 3) S5B	54.9	50.0	58.1	43.8	64.1	0.47	0.08	51
*k*NN *(k* = 3) SEL	56.3	39.3	67.4	44.0	63.0	0.42	0.07	60
SVM (linear) S5B	53.5	50.0	55.8	42.4	63.2	0.46	0.06	63
SVM (linear) SEL	53.5	50.0	55.8	42.4	63.2	0.46	0.06	64
SVM (poly = 5) RFE	52.1	46.4	55.8	40.6	61.5	0.43	0.02	78
SVM (linear) RFE	52.1	39.3	60.5	39.3	60.5	0.39	0.00	85
*k*NN *(k* = 3) RFE	50.7	35.7	60.5	37.0	59.1	0.36	-0.04	97
SVM (poly = 5) S5B	49.3	39.3	55.8	36.7	58.5	0.38	-0.05	100
*k*NN *(k* = 5) S5B	47.9	35.7	55.8	34.5	57.1	0.35	-0.08	109
*k*NN *(k* = 5) RFE	46.5	35.7	53.5	33.3	56.1	0.34	-0.11	119

Compared to straight walking, turn data had better faller classification (Table 5.2). The best turn-based combination was RF S5B, with 77.5% accuracy, 67.9% sensitivity, 83.7% specificity, and 0.52 MCC score. The second best results, obtained using RF SEL, were similar to RF S5B.

Table 5.2. Turn section 5FCV results. PPV: positive predictive value, NPV: negative predictive value, MCC: Matthews correlation coefficient, S5B: select-5-best method, SEL: false positive and discovery rate method, RFE: recursive feature eliminator, RF: random forest, *k*NN: *k*-nearest neighbour, SVM: support vector machine, linear: linear kernel, poly: polynomial kernel.

Classifier, Feature Selector	Accuracy (%)	Sensitivity (%)	Specificity (%)	PPV (%)	NPV (%)	F1 Score	MCC	Rank Sum
RF S5B	77.5	67.9	83.7	73.1	80.0	0.70	0.52	12
RF SEL	77.5	64.3	86.0	75.0	78.7	0.69	0.52	14
RF RFE	69.0	53.6	79.1	62.5	72.3	0.58	0.34	38
*k*NN (*k* = 5) SEL	69.0	50.0	81.4	63.6	71.4	0.56	0.33	45
*k*NN (*k*= 5) S5B	71.8	42.9	90.7	75.0	70.9	0.55	0.39	46
SVM (linear) S5B	67.6	53.6	76.7	60.0	71.7	0.57	0.31	50
SVM (linear) SEL	66.2	57.1	72.1	57.1	72.1	0.57	0.29	55
KNN (k = 3) S5B	67.6	50.0	79.1	60.9	70.8	0.55	0.30	57
SVM (poly = 3) RFE	62.0	67.9	58.1	51.4	73.5	0.58	0.25	58
kNN (k =3) SEL	66.2	50.0	76.7	58.3	70.2	0.54	0.28	70
SVM (poly = 3) SEL	60.6	64.3	58.1	50.0	71.4	0.56	0.22	73
SVM (poly = 5) SEL	54.9	78.6	39.5	45.8	73.9	0.58	0.19	76
SVM (poly = 5) S5B	60.6	60.7	60.5	50.0	70.3	0.55	0.21	81
*k*NN (*k* = 5) RFE	63.4	35.7	81.4	55.6	66.0	0.43	0.19	89
SVM (linear) RFE	60.6	50.0	67.4	50.0	67.4	0.50	0.17	94
SVM (poly = 3) S5B	59.2	57.1	60.5	48.5	68.4	0.52	0.17	97
*k*NN (*k* = 3) RFE	62.0	39.3	76.7	52.4	66.0	0.45	0.17	98
SVM (poly = 5) RFE	57.7	46.4	65.1	46.4	65.1	0.46	0.12	114

RF, 3NN, and 5NN, and linear and third order polynomial SVM classifiers performed best in Test I. The worst performing classifier was the fifth degree polynomial SVM, which appeared only once in the top-nine combinations for the straight data and not at all for the turn data. S5B and SEL feature selectors performed better than RFE using the same classifier models. The worst feature selector was the RFE, which appeared four times, compared to seven times for S5B and SEL methods. Based on these results, the fifth order polynomial SVM classifier and RFE selector were eliminated from further tests. Therefore, RF, 3NN, 5NN, and linear and third order polynomial SVM classifiers, and S5B and SEL feature selectors were used for Test II, for both turn and straight datasets.

5.3.2 Test II

5.3.2.1 Classification Results

Faller classification results for Test II (Tables 5.3 and 5.4) were similar to Test I. Faller classification with turn data (Table 5.4) outperformed straight walking data (Table 5.3). The best turn-based combination (RF S5B) had 73.4% accuracy, 60.5% sensitivity, 82.0% specificity, and 0.44 MCC score. The best straight-walking-based combination (3NN S5B) had 55.5% accuracy, 46.1% sensitivity, 61.8% specificity and 0.08 MCC score.

5.3.2.2 Most Frequently Occurring Feature Results

Frequency plots of 2500-RSS selected features for straight walking, using S5B and SEL, are shown in Figures 5.3 and 5.4, respectively. The most frequently occurring S5B features, in descending order of frequency, were: maximum of SD of anterior RS acceleration (index 11), SD of maximum posterior LS acceleration (index 255), minimum of SD of anterior RS acceleration (index 85), mean of SD anterior RS acceleration (index 159), SD of mean inferior LB acceleration (index 285), mean of mean anterior RS acceleration (index 158), maximum of SD anterior LB acceleration (index 61), maximum of maximum anterior LB acceleration (index 62), maximum of mean anterior RS acceleration (index 10), maximum of mean anterior LB acceleration (index 60), SD of SD inferior LB acceleration (index 286), mean of maximum anterior LB acceleration (index 210), SD of mean anterior LB acceleration (index 282), and SD of mean posterior LS acceleration (index 253). These features were also the top features for the SEL method; however, SEL frequencies were lower overall and frequency ordering was not the same.

Table 5.3. Straight-walking section results for 2500-RSS CV, ordered by ranked performance. PPV: positive predictive value, NPV: negative predictive value, MCC: Matthews correlation coefficient, S5B: select-5-best method, SEL: false positive and discovery rate method, RFE: recursive feature eliminator, RF: random forest, *k*NN: *k*-nearest neighbour, SVM: support vector machine, linear: linear kernel, poly: polynomial kernel, $\bar{x}$: mean, SD: standard deviation, CI: 95% confidence interval.

Classifier, Feature Selection	Accuracy (%)			Sensitivity (%)			Specificity (%)			PPV (%)			NPV (%)			F1			MCC		
	$\bar{x}$	SD	CI	$\bar{x}$	SD	CI	$\bar{x}$	SD	CI	$\bar{x}$	SD	CI	$\bar{x}$	SD	CI	$\bar{x}$	SD	CI	$\bar{x}$	SD	CI
*k*NN (*k* = 3) S5B	55.5	12.0	0.47	46.1	21.2	0.83	61.8	16.2	0.64	44.6	16.9	0.66	63.2	11.5	0.45	0.45	0.17	0.007	0.08	0.26	0.010
RF S5B	56.2	11.4	0.45	39.8	20.3	0.80	67.2	15.9	0.62	44.7	19.6	0.77	62.6	9.9	0.39	0.42	0.18	0.007	0.07	0.26	0.010
RF SEL	56.9	11.2	0.44	34.5	20.3	0.79	71.9	18.3	0.72	45.0	25.2	0.99	62.2	8.7	0.34	0.39	0.18	0.007	0.07	0.30	0.012
SVM (poly = 3) SEL	51.7	11.1	0.43	59.7	33.6	1.32	46.4	30.3	1.19	42.6	18.8	0.74	63.3	25.6	1.00	0.50	0.20	0.008	0.06	0.39	0.015
*k*NN (*k* = 5) S5B	55.0	11.8	0.46	43.6	21.8	0.85	62.7	17.0	0.67	43.8	18.3	0.72	62.5	11.2	0.44	0.44	0.18	0.007	0.06	0.26	0.010
SVM (linear) SEL	53.4	12.1	0.48	50.3	23.7	0.93	55.5	23.7	0.93	43.0	17.3	0.68	62.6	15.9	0.62	0.46	0.16	0.006	0.06	0.30	0.012
SVM (linear) S5B	50.9	11.9	0.47	53.6	25.4	0.99	49.1	19.3	0.76	41.3	15.0	0.59	61.4	16.4	0.64	0.47	0.17	0.007	0.03	0.27	0.011
*k*NN (*k* = 3) SEL	54.0	11.4	0.45	37.5	19.9	0.78	65.1	17.3	0.68	41.7	19.6	0.77	61.0	9.7	0.38	0.39	0.17	0.007	0.03	0.25	0.010
SVM (poly = 3) S5B	48.7	10.4	0.41	61.6	33.6	1.32	40.1	26.2	1.03	40.7	16.1	0.63	61.0	26.4	1.03	0.49	0.20	0.008	0.02	0.35	0.014
*k*NN (*k* = 5) SEL	53.8	10.8	0.42	34.6	19.9	0.78	66.6	17.7	0.69	40.8	20.5	0.80	60.4	9.2	0.36	0.37	0.17	0.007	0.01	0.26	0.010

Table 5.4. Turn section results for 2500-RSS CV, ordered by ranked performance. PPV: positive predictive value, NPV: negative predictive value, MCC: Matthews correlation coefficient, S5B: select-5-best method, SEL: false positive and discovery rate method, RFE: recursive feature eliminator, RF: random forest, *k*NN: *k*-nearest neighbour, SVM: support vector machine, linear: linear kernel, poly: polynomial kernel, $\bar{x}$: mean, SD: standard deviation, CI: 95% confidence interval.

Classifier, Feature Selector	Accuracy (%)			Sensitivity (%)			Specificity (%)			PPV (%)			NPV (%)			F1			MCC		
	$\bar{x}$	SD	CI	$\bar{x}$	SD	CI	$\bar{x}$	SD	CI	$\bar{x}$	SD	CI	$\bar{x}$	SD	CI	$\bar{x}$	SD	CI	$\bar{x}$	SD	CI
RF S5B	73.4	10.6	0.42	60.5	20.5	0.81	82.0	12.8	0.50	69.1	18.2	0.71	75.7	10.2	0.40	0.65	0.17	0.007	0.44	0.24	0.009
RF SEL	71.6	10.9	0.43	58.3	20.7	0.81	80.4	13.3	0.52	66.5	18.5	0.72	74.3	10.3	0.41	0.62	0.17	0.007	0.40	0.24	0.010
k NN (*k* = 5) S5B	69.2	11.2	0.44	49.0	21.4	0.84	82.7	13.3	0.52	65.3	22.5	0.88	70.8	9.7	0.38	0.56	0.19	0.008	0.34	0.27	0.011
k NN (*k* = 3) S5B	68.0	11.2	0.44	50.8	20.7	0.81	79.6	13.9	0.55	62.4	20.9	0.82	70.8	9.8	0.39	0.56	0.18	0.007	0.32	0.26	0.010
SVM (linear) S5B	66.7	11.7	0.46	57.6	20.8	0.82	72.8	16.0	0.63	58.5	17.7	0.69	72.0	11.7	0.46	0.58	0.16	0.006	0.30	0.25	0.010
SVM (linear) SEL	64.7	13.0	0.51	57.6	24.2	0.95	69.5	17.9	0.70	55.7	19.3	0.76	71.1	14.4	0.56	0.57	0.19	0.007	0.27	0.31	0.012
k NN (*k* = 5) SEL	67.2	12.5	0.49	48.7	21.6	0.85	79.5	14.9	0.58	61.3	23.2	0.91	69.9	10.5	0.41	0.54	0.20	0.008	0.30	0.29	0.012
k NN (*k* = 3) SEL	66.8	12.7	0.50	50.0	21.3	0.83	78.0	15.2	0.60	60.3	22.2	0.87	70.1	10.8	0.42	0.55	0.19	0.008	0.29	0.29	0.011
SVM (poly = 3) SEL	61.8	13.1	0.51	50.7	25.3	0.99	69.2	24.8	0.97	52.3	25.1	0.98	67.8	15.4	0.61	0.51	0.18	0.007	0.20	0.33	0.013
SVM (poly = 3) S5B	60.7	13.8	0.54	55.7	23.6	0.93	64.1	22.3	0.87	50.8	20.0	0.78	68.4	15.8	0.62	0.53	0.17	0.007	0.20	0.30	0.012

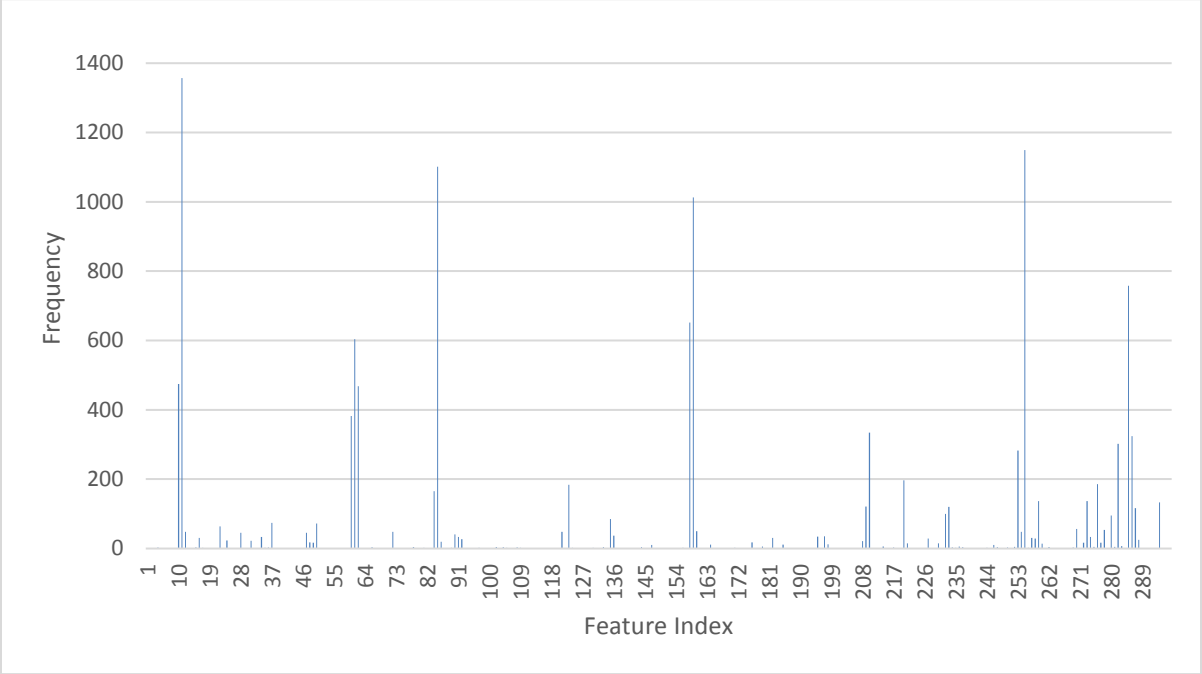

Figure 5.3. Histogram of selected straight-walking data features using select-5-best (S5B) feature selection.

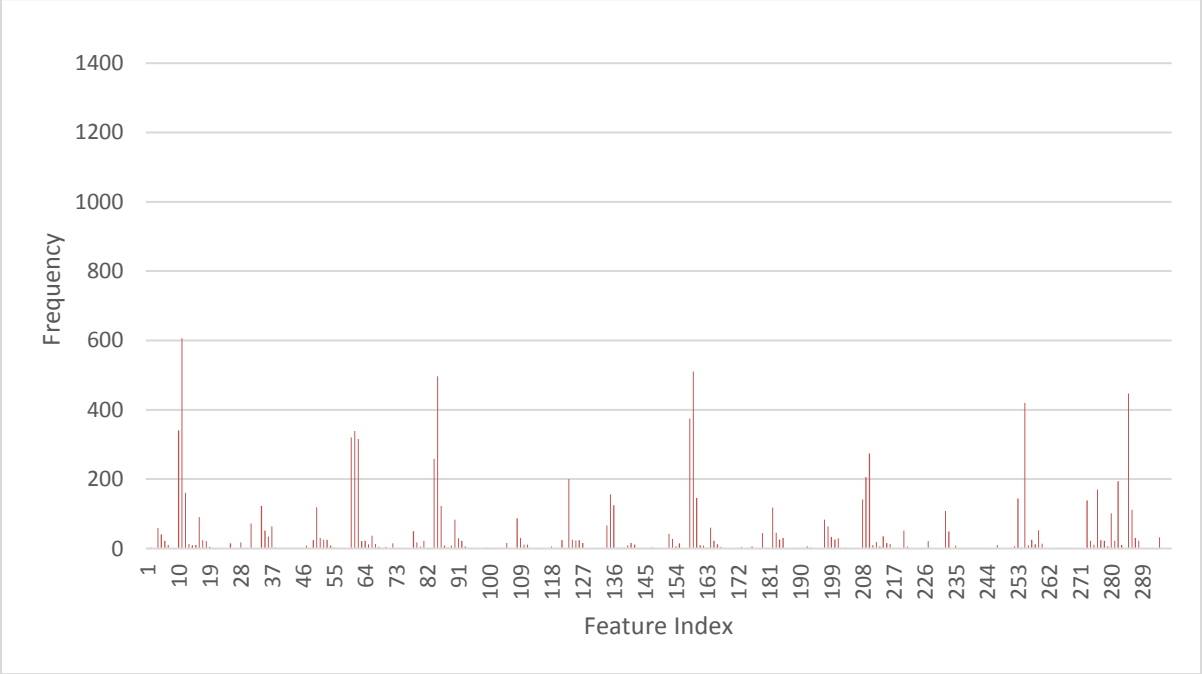

Figure 5.4. Histogram of selected straight-walking data features using SEL feature selection.

Frequency plots of 2500-RSS selected features for turns, using S5B and SEL, are shown in Figures 5.5 and 5.6, respectively. The most frequently occurring turn based features for the S5B method, in descending order of frequency, were: minimum of anterior-posterior REOH for RS (index 96), SD of SD anterior LS acceleration (index 257), SD of mean anterior LS acceleration (index 256), maximum of medial-lateral FQFFT for LB (index 70), maximum of anterior-posterior FQFFT for LB (index 69), SD of maximum anterior LS acceleration (index 258), SD of vertical FQFFT for RS (index 243), maximum of vertical FQFFT for LS (index 45), and maximum of anterior-posterior FQFFT for LS (index 43). These features were also selected most frequently by the SEL method, though frequency ordering was slightly different.

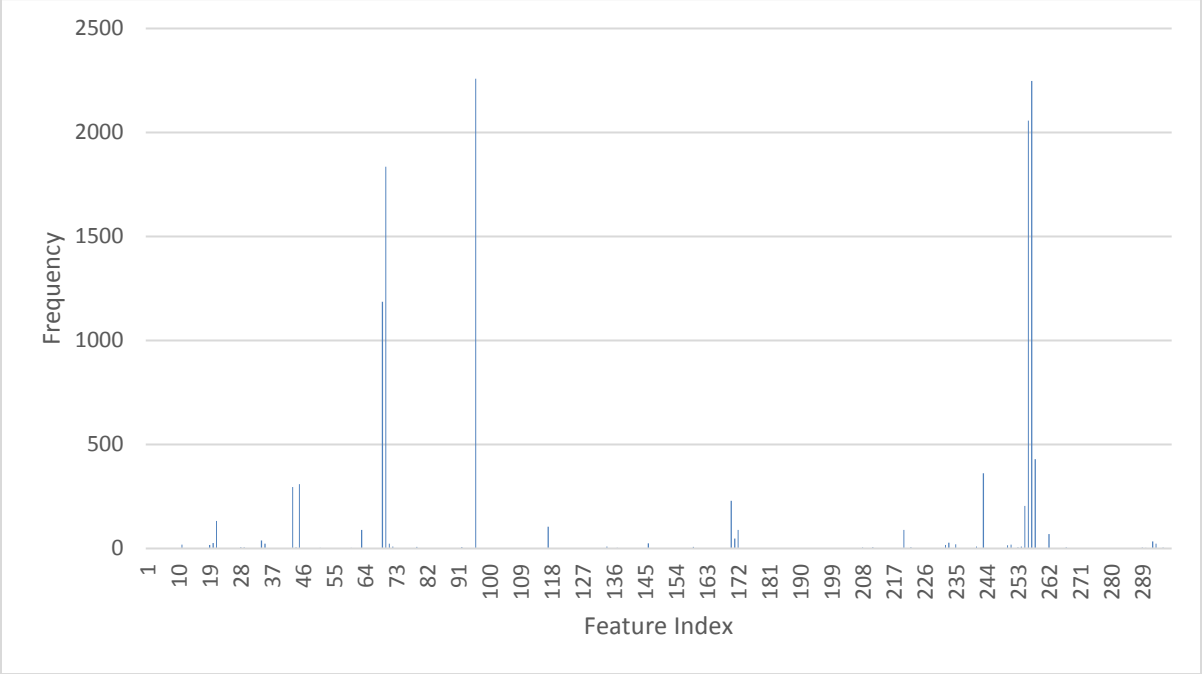

Figure 5.5. Histogram of selected turn data features using select-5-best (S5B) feature selection.

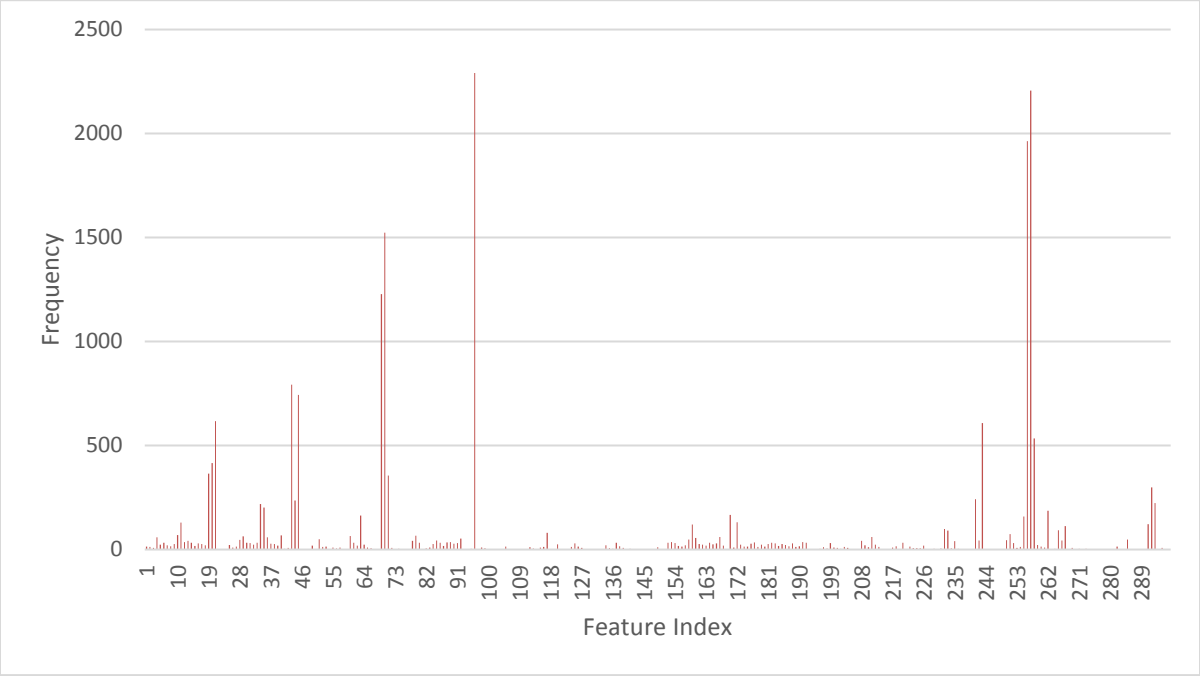

Figure 5.6. Histogram of selected turn data features using SEL feature selection.

5.3.3 Test III

The best results for straight walking (Table 5.5) were for the 5 MFO feature subset (maximum of SD of anterior RS acceleration, SD of maximum posterior LS acceleration, minimum of SD of anterior RS acceleration, mean of SD anterior RS acceleration, SD of mean inferior LB acceleration), with 64.1% accuracy, 59.9% sensitivity, 66.9% specificity, and 0.26 MCC score. For turn walking (Table 5.6), the best results were for the 5 MFO feature subset (minimum of anterior-posterior REOH for RS, SD of SD anterior LS acceleration, SD of mean anterior LS acceleration, maximum of medial-lateral FQFFT for LB, maximum of anterior-posterior FQFFT for LB), with 77.3% accuracy, 66.1% sensitivity, 84.7% specificity, and 0.52 MCC score. The Test III results were generally superior to those of Test II, where all accuracies of Test III were higher than for Test II.

Table 5.5. Most frequently occurring (MFO) feature subsets for straight-walking section results and 3NN classifier using 2500-RSS CV, ordered by ranked performance. PPV: positive predictive value, NPV: negative predictive value, MCC: Matthews correlation coefficient, $\bar{x}$: mean, SD: standard deviation, CI: 95% confidence interval.

# Features	Accuracy (%)			Sensitivity (%)			Specificity (%)			PPV (%)			NPV (%)			F1			MCC		
	$\bar{x}$	SD	CI	$\bar{x}$	SD	CI	$\bar{x}$	SD	CI	$\bar{x}$	SD	CI	$\bar{x}$	SD	CI	$\bar{x}$	SD	CI	$\bar{x}$	SD	CI
5	64.1	10.8	0.42	59.9	19.2	0.75	66.9	14.5	0.57	54.7	14.3	0.56	71.4	11.0	0.43	0.57	0.14	0.006	0.26	0.23	0.009
3	63.1	11.3	0.44	61.2	20.0	0.78	64.4	14.9	0.59	53.4	14.0	0.55	71.3	11.9	0.47	0.57	0.15	0.006	0.25	0.24	0.009
4	62.2	10.8	0.42	57.7	18.9	0.74	65.2	15.0	0.59	52.5	14.6	0.57	69.8	10.7	0.42	0.55	0.14	0.006	0.23	0.23	0.009
9	61.5	10.4	0.41	42.1	18.8	0.74	74.5	14.0	0.55	52.4	20.0	0.79	65.9	8.5	0.33	0.47	0.17	0.007	0.17	0.24	0.009
10	60.7	11.1	0.43	44.7	19.9	0.78	71.4	14.6	0.57	51.1	19.1	0.75	66.0	9.5	0.37	0.48	0.17	0.007	0.17	0.25	0.010
6	60.6	12.3	0.48	56.1	20.1	0.79	63.6	16.7	0.66	50.7	16.0	0.63	68.5	12.2	0.48	0.53	0.16	0.006	0.20	0.26	0.010
2	60.0	11.5	0.45	57.2	19.3	0.76	61.8	15.9	0.62	50.0	14.5	0.57	68.4	11.7	0.46	0.53	0.15	0.006	0.19	0.24	0.009
8	60.6	10.3	0.40	38.5	18.7	0.73	75.4	13.8	0.54	51.1	21.6	0.85	64.8	8.2	0.32	0.44	0.17	0.007	0.15	0.25	0.010
11	59.6	11.1	0.43	41.9	19.4	0.76	71.4	14.9	0.59	49.4	19.7	0.77	64.8	9.3	0.37	0.45	0.17	0.007	0.14	0.25	0.010
7	59.2	11.2	0.44	44.0	18.8	0.74	69.3	15.1	0.59	48.9	18.6	0.73	65.0	9.4	0.37	0.46	0.16	0.006	0.14	0.24	0.010
1	57.0	11.0	0.43	50.2	20.1	0.79	61.5	15.7	0.62	46.5	14.8	0.58	64.9	10.9	0.43	0.48	0.15	0.006	0.12	0.24	0.009
13	57.8	10.9	0.43	37.4	19.1	0.75	71.4	14.5	0.57	46.6	20.4	0.80	63.1	8.9	0.35	0.41	0.17	0.007	0.09	0.25	0.010
14	57.6	10.5	0.41	37.6	18.9	0.74	70.9	14.5	0.57	46.3	19.7	0.77	63.0	8.5	0.33	0.42	0.17	0.007	0.09	0.24	0.010
12	57.0	10.5	0.41	36.5	19.1	0.75	70.6	14.0	0.55	45.3	20.2	0.79	62.5	8.5	0.33	0.40	0.17	0.007	0.07	0.25	0.010

Table 5.6. Most frequently occurring (MFO) feature subsets for turn section results and RF classifier using 2500-RSS CV, ordered by ranked performance. PPV: positive predictive value, NPV: negative predictive value, MCC: Matthews correlation coefficient, $\bar{x}$: mean, SD: standard deviation, CI: 95% confidence interval.

# Features	Accuracy (%)			Sensitivity (%)			Specificity (%)			PPV (%)			NPV (%)			F1			MCC		
	$\bar{x}$	SD	CI	$\bar{x}$	SD	CI	$\bar{x}$	SD	CI	$\bar{x}$	SD	CI	$\bar{x}$	SD	CI	$\bar{x}$	SD	CI	$\bar{x}$	SD	CI
5	77.3	9.1	0.36	66.1	19.6	0.77	84.7	11.4	0.45	74.3	15.5	0.61	79.0	9.7	0.38	0.70	0.15	0.006	0.52	0.20	0.008
6	77.1	9.4	0.37	66.2	19.5	0.76	84.4	11.7	0.46	73.9	15.9	0.62	78.9	9.7	0.38	0.70	0.15	0.006	0.52	0.21	0.008
3	77.0	9.6	0.38	67.7	18.9	0.74	83.2	12.2	0.48	72.9	15.7	0.62	79.5	9.7	0.38	0.70	0.14	0.006	0.52	0.21	0.008
9	76.3	9.6	0.38	63.3	19.8	0.78	84.9	11.6	0.46	73.6	16.7	0.66	77.6	9.6	0.38	0.68	0.15	0.006	0.50	0.22	0.009
2	76.4	9.4	0.37	65.9	18.9	0.74	83.4	12.0	0.47	72.6	15.8	0.62	78.6	9.6	0.38	0.69	0.14	0.006	0.50	0.20	0.008
7	75.8	9.6	0.38	62.4	19.5	0.76	84.7	12.0	0.47	73.2	16.7	0.66	77.2	9.5	0.37	0.67	0.15	0.006	0.49	0.21	0.008
8	75.7	9.7	0.38	62.4	19.7	0.77	84.5	12.0	0.47	72.9	16.9	0.66	77.1	9.6	0.38	0.67	0.15	0.006	0.48	0.22	0.009
4	75.5	9.5	0.37	63.3	19.5	0.76	83.7	11.9	0.47	72.2	16.5	0.65	77.4	9.6	0.38	0.67	0.15	0.006	0.48	0.21	0.008
1	75.3	9.4	0.37	61.5	19.5	0.76	84.6	11.7	0.46	72.7	16.8	0.66	76.7	9.3	0.36	0.67	0.15	0.006	0.48	0.21	0.008

5.4 Discussion

A new method for faller classification in older adults was developed using walking-turn accelerometer-based features extracted from wearable sensor data. This research confirmed that turn features performed better than straight walking features for prospective faller classification, and the best overall classification method used a random forest classifier and five turn-based features, obtained from the S5B feature selection process.

To promote classification generalizability and reliability, and to avoid methodological problems associated with validation and training-testing protocols seen in the fall-risk assessment literature [40], two stratified cross-validation methods were used. The top classifiers and feature selectors were chosen in Test I using 5FCV and then used for Test II, which used 2500-RSS CV. The 2500-RSS, used for Tests II and III, generated viable mean results, based on the law of large numbers [78] and narrow 95% confidence intervals, indicating that the mean values were likely similar to population values.

Test I determined that turn features performed better than straight walking features for prospective faller classification since turn-based models had greater accuracy, sensitivity, specificity, F1-score, and MCC than straight-walking models. Test II reinforced the conclusions from Test I, since turn features also outperformed straight walking features for faller classification. The best turn-based classifier-feature selector combination (RF-S5B) had results that were at least 24% greater than corresponding straight-walking results, with the worst turn-based classifier outperforming the best straight-walking-based classifier. The narrow confidence intervals, which were less than ±1% for turn classification performance metrics and ±1.32% for straight walking, support the generalizability of these results for population-based applications.

Test III determined that, for turns, the best feature subset included minimum of anterior-posterior REOH for right shank, SD of SD anterior left shank acceleration, SD of mean anterior left shank acceleration, maximum of medial-lateral FQFFT for lower back, and maximum of anterior-posterior FQFFT for lower back. Feature maxima, minima, and SD appeared more often in the best feature subset than mean-based features. This further confirmed that extreme values (maximum and minimum) and variability (SD) provide better discriminative information for turns, as found in previous research [51].

The most frequently occurring turn feature in the feature selection process (Test II) was minimum anterior-posterior REOH for the right shank, which composed the 1 MFO feature subset. Interestingly, only modest differences occurred between the 1 MFO feature subset and the best feature subset (5 MFO Feature). The strong performance using only the minimum-AP-REOH-right-shank feature indicates the importance of this feature for faller classification. This result is supported by [7,45–49,79] , where a small REOH indicated step-to-step asymmetry within strides and possibly gait instability. Two features in the 5 MFO feature subset involved the lower back sensor maximum FQFFT, across all turn sections for the anterior-posterior and medial-lateral axes. A low FQFFT value indicates more high frequency than low frequency components. Walking can be associated with activities linked to decreased stability [23] and higher frequency components indicate less steady movements [11,44] and possibly sudden movements to recover balance; therefore, frequency components at the lower back may be useful for faller classification. The remaining 5 MFO features for turn data were related to SD across different turn sections, suggesting that acceleration variation over time can be a good indicator for faller classification.

Previous approaches that used turn-walking to discriminate fallers and non-fallers have used the TUG test [17,19–21,80]. However, a meta-analysis of 53 studies suggested that TUG was ineffective for determining fall risk for healthy older individuals [37]. This was primarily due to variations in the thresholds across studies used to classify fallers and non-fallers. Since this study included multiple turn sections and found that classification using turn-based features performed better than using straight-walking features, the methods of this study may be a more suitable alternative than the TUG for prospectively classifying fallers.

Existing elderly fall screening assessments could benefit by better prospective faller classification. The results of this research suggest that integrating wearable-sensor turn-based features and machine learning in elderly screening assessments may improve faller identification. Since a shorter test might be easier to administer in a clinical setting, future research could study whether a shorter distance with fewer turns could also be effective.

Chapter 6
Conclusions

This chapter provides an overview of results and conclusions from the research described in previous chapters of this thesis. Furthermore, it revisits objectives set out in Section 1.2. Future work and recommendations for the fall-risk assessment field are presented and discussed.

6.1 Observations and Review of Objectives

This thesis presented comprehensive comparisons assessing the usefulness of turn and straight walking wearable-sensor-based features for faller status (faller, non-faller) classification. Turns and straight sections were segmented, with features extracted and summary features created for each participant.

Overlapping conclusions drawn from statistical analysis and classification models confirm that the turn-based features have stronger classification and predictive power than the corresponding straight-walking based features. The feature set with significantly different mean values between faller and non-faller groups included solely turn based features and four out of five of these features were shared with the five MFO features, which provided the best classification results (Chapter 5). Future research should consider a combined set of six of the most important features: minimum of anterior-posterior REOH for right shank, SD of SD anterior left shank acceleration, SD of mean anterior left shank acceleration, maximum of medial-lateral FQFFT for lower back, and maximum of anterior-posterior FQFFT for lower back (only found for 5 MFO) and SD of maximum anterior left shank acceleration (only found in statistical analysis).

Wearable sensors such as accelerometers are easy to apply on people, require minimal calibration, and are low cost, making the methods investigated a viable option for fall-risk assessment. Since turn based features outperformed straight walking based features for prospective faller classification, assessments should include multiple turns. Using multiple turns allows calculation of SD, maxima and minima of the extracted features over time and these were found to be strong features for turn data classification in this thesis. SD, maxima and minima have been found to be important for previous fall risk assessment research [12,51].

The objectives presented in Section 1.2 were satisfied as follows:

Segment turn straight walking sections from 6MWT acceleration data and extract features

A novel method for segmenting turn sections from multiple tri-axial accelerometers was developed. Using decreases in magnitude of vertical acceleration peaks, the method determined the location of all turns within a participant's 6MWT data. Delimiting the start and end of a turn was achieved. With a limited portion of the signal to search for a minimum peak amplitude, the second part of the algorithm found the central footstep of a turn, which corresponded with either the right or left foot, and was then able to find the two steps before and after the central step and set these footfalls, plus a small buffer as the limits of the turn. Certain instances occurred where the segmentation did not work as intended. Failure modes were limited to excessive noise in the source data or what appeared to be a non-standard turning methods (i.e., no central-step or no drop in peak amplitude). These failures were limited to a small number of participant's and only involved a small percentage of those participant's turns.

Perform statistical analysis on accelerometer-based features from turn-walking and straight-walking sections of the 6MWT performed by older adults

This study presented a statistical comparison of turn and straight walking accelerometer-based features from the 6MWT. Most features had significant differences ($p < 0.05$), between turn and straight walking modes, for both faller and non-faller groups, with some turn features values linked to fall risk. The statistical analysis comparing features for faller status (prospective faller, non-faller), with turn and straight features treated separately, showed that turn features had significant differences ($p < 0.05$) between the two faller status groups, whereas straight-walking features did not show statistical differences. The five turn based features that were significantly different between PF and NF groups were minimum of anterior-posterior REOH for right shank, SD of SD anterior left shank acceleration, SD of mean anterior left shank acceleration, maximum of medial-lateral FQFFT for lower back, and SD of maximum anterior left shank acceleration. Future research could determine if these accelerometer-based features provide generalizable faller prediction results with different turn datasets.

Develop and compare faller prediction models using walking-turn and straight-walking accelerometer-based features

A novel wearable-sensor based faller classification method using walking-turns was developed. This work is the first to directly compare prospective classification results using straight and turn walking data, based on wearable-accelerometer measures. A marked improvement in all classification performance metrics occurred when turn data was used for faller classification, compared to straight walking data. Turn data acquired from accelerometers contains useful biomechanical information that can improve prospective fall risk classification for healthy older adults. A random forest classifier paired with a Select-5-best (S5B) feature selector provided the best classification results for both turn and straight walking data. The most frequently occurring turn feature in the feature selection process was minimum anterior-posterior REOH for the right shank, which composed the 1 MFO Feature subset and produced comparable results to the 5 MFO Feature subset, indicating the importance of this feature for faller classification. Future work could examine the effectiveness of the most frequently selected, best performing turn features on faller classification in other populations.

The best turn-based combination (RF S5B) had 73.4% accuracy, 60.5% sensitivity, 82.0% specificity, and 0.44 MCC score. The 5 MFO features selected from a 2500-RSS cross validation from a the S5B feature selector were minimum of anterior-posterior REOH for RS, SD of SD anterior LS acceleration, SD of mean anterior LS acceleration, maximum of medial-lateral FQFFT for LB and maximum of anterior-posterior FQFFT for LB. Using these features provided classification results of 77.3% accuracy, 66.1% sensitivity, 84.7% specificity, and 0.52 MCC score. However, these results should be taken only as an indicator of the importance of the features, since the feature selection was not based solely on training data, in contrast to the RF S5B classifier-model – feature-selection combination.

6.2 Future Work and Recommendations

This thesis presented a turn segmentation method for acceleration data and analysed the ability of turn or straight walking features from acceleration data to classify fallers. The turn segmentation algorithm, while successful, was specific to the methodology. A turn was defined

using a fixed number of steps. While this standardized the analysis, this method may have led to one or two extra or missed steps for a participant's turn. The data was recorded by accelerometers rather than accelerometers paired with gyroscopes, as in inertial measurement units (IMU). Gyroscopes measure rotation about a given axis and could greatly simplify turn segmentation since a turn could be delineated using the rate of turning. Alternatively, video synchronized with accelerometer data or manually marking turns by time could be employed. These methods could additionally avoid the use of a fixed number of steps for a turn.

A closer examination of misclassified participant data sets could provide insight into how and why these data were misclassified. Projecting data into a lower dimensions (dimension ≤ 3) could allow for a more intuitive and visual interpretation of the data. This representation could be achieved by limiting the number of features or using a dimensionality reduction technique such as *t*-distributed stochastic neighbor embedding (*t*-SNE) [81] or principal component analysis. Another method to further analyse the data would be to examine misclassified examples on a feature by feature basis. By determining which features caused an example to be misclassified, feature engineering or examination of new features could be explored toward correcting or compensating for misclassification. Additionally, if a misclassified example had a feature that differentiated it from the other class, but this feature was eliminated during feature selection, this case could be examined and accounted for.

Future faller classification and fall risk assessment research could augment the wearable sensors feature sets with contextual information about participants, such as age, sex, height, weight, fear of falling. Feature analysis or selection would determine if these factors are useful. Additional turn-based features that should be incorporated into faller classification models include features shown in the literature to have significant effects, such as rate of turn, duration of turn, and number of steps. These features could be extracted from gyroscope data. Gyroscope data could additionally provide similar features to those discussed in this thesis, such as frequency domain features, and raw velocity measurements during turns. The fall occurrence classification criterion could also have an added degree of granularity by incorporating the number of times a participant had fallen. This could be combined with probabilistic classification models such as Logistic Regression or Neural Networks using softmax output layers to provide

not just a classification of faller or non-faller but a probability of falling, which may be better suited for clinical assessments and treatment.

References

1. Davis JC, Robertson MC, Ashe MC, Liu-Ambrose T, Khan KM, Marra CA. International comparison of cost of falls in older adults living in the community: A systematic review. Osteoporosis International. 2010;21: 1295–1306.

2. Englander F, Terregrossa RA, Hodson TJ. Economic dimensions of slip and fall injuries. Journal of Forensic Science. 1996;41: 733–746.

3. El-Khoury F, Cassou B, Charles M-A, Dargent-Molina P. The effect of fall prevention exercise programmes on fall induced injuries in community dwelling older adults: Systematic review and meta-analysis of randomised controlled trials. BMJ. 2013;347: f6234.

4. Tinetti ME. Preventing falls in elderly persons. New England Journal of Medicine. 2003;348: 42–49.

5. Rao SS. Prevention of falls in older patients. American Family Physician. 2005;72: 81–88.

6. Özdemir AT, Barshan B. Detecting Falls with Wearable Sensors Using Machine Learning Techniques. Sensors. 2014;14: 10691–10708.

7. Howcroft J, Lemaire ED, Kofman J. Wearable-sensor-based classification models of faller status in older adults. PLoS One. 2016;11: e0153240.

8. Howcroft J, Kofman J, Lemaire ED. Review of fall risk assessment in geriatric populations using inertial sensors. Journal of Neuroengineering and Rehabilitation. 2013;10(91).

9. Ejupi A, Lord SR, Delbaere K. New methods for fall risk prediction. Current Opinion in Clinical Nutrition and Metabolic Care. 2014;17: 407–411.

10. Tax DM, Duin RP. Feature scaling in support vector data descriptions. Learning from Imbalanced Datasets. 2000; 25–30.

11. Doheny EP, Walsh C, Foran T, Greene BR, Fan CW, Cunningham C, Kenny RA. Falls classification using tri-axial accelerometers during the five-times-sit-to-stand test. Gait and Posture. 2013;38: 1021–1025.

12. Mancini M, Schlueter H, El-Gohary M, Mattek N, Duncan C, Kaye J, Horak FB. Continuous monitoring of turning mobility and its association to falls and cognitive function: A pilot study. The Journals of Gerontology Series A: Biological Sciences and Medical Sciences. 2016;71(8): 1102-1108.

13. Segal AD, Orendurff MS, Czerniecki JM, Shofer JB, Klute GK. Local dynamic stability in turning and straight-line gait. Journal of Biomechanics. 2008;41: 1486–1493.

14. Fino PC, Frames CW, Lockhart TE. Classifying step and spin turns using wireless gyroscopes and implications for fall risk assessments. Sensors. 2015;15: 10676–10685.

15. Justine M, Manaf H, Sulaiman A, Razi S, Alias HA. Sharp turning and corner turning: Comparison of energy expenditure, gait parameters, and level of fatigue among community-dwelling elderly. BioMed Research International. 2014;2014.

16. Glaister BC, Bernatz GC, Klute GK, Orendurff MS. Video task analysis of turning during activities of daily living. Gait and Posture. 2007;25: 289–294.

17. Greene BR, O'Donovan A, Romero-Ortuno R, Cogan L, Scanaill CN, Kenny RA. Quantitative falls risk assessment using the Timed Up and Go Test. IEEE Transactions on Biomedical Engineering. 2010;57: 2918–2926.

18. Dite W, Temple VA. A clinical test of stepping and change of direction to identify multiple falling older adults. Archives of Physical Medicine and Rehabilitation. 2002;83: 1566–1571.

19. Dite W, Temple VA. Development of a clinical measure of turning for older adults. American Journal of Physical Medicine and Rehabilitation. 2002;81: 857–866.

20. Thigpen MT, Light KE, Creel GL, Flynn SM. Turning difficulty characteristics of adults aged 65 years or older. Physical Therapy. 2000;80: 1174–1187.

21. Skrba Z, O'Mullane B, Greene BR, Scanaill CN, Fan CW, Quigley A, Nixon P. Objective real-time assessment of walking and turning in elderly adults. 2009 Annual International Conference of the IEEE Engineering in Medicine and Biology Society. IEEE; 2009. pp. 807–810.

22. Guyatt GH, Sullivan MJ, Thompson PJ, Fallen EL, Pugsley SO, Taylor DW, Berman LB. The 6-minute walk: A new measure of exercise capacity in patients with chronic heart failure. Canadian Medical Association Journal. 1985;132: 919-923.

23. Howcroft J, Kofman J, Lemaire ED, McIlroy WE. Analysis of dual-task elderly gait in fallers and non-fallers using wearable sensors. Journal of Biomechanics. 2016;49: 992–1001.

24. Thorpe KE. The rise in health care spending and what to do about it. Health Affairs. 2005;24: 1436–1445.

25. Hagist C, Kotlikoff L. Who's going broke? Comparing growth in healthcare costs in ten OECD countries. National Bureau of Economic Research; 2005.

26. Centers for Disease Control and Prevention (CDC). Trends in aging--United States and worldwide. Morbidity and Mortality Weekly Report. 2003;52: 101–104, 106.

27. Sattin RW. Falls among older persons: A public health perspective. Annual Review of Public Health. 1992;13: 489–508.

28. Hausdorff JM, Rios DA, Edelberg HK. Gait variability and fall risk in community-living older adults: A 1-year prospective study. Archives of Physical Medicine and Rehabilitation. 2001;82: 1050–1056.

29. Maki BE, Sibley KM, Jaglal SB, Bayley M, Brooks D, Fernie GR, Flint AJ, Gage W, Liu BA, McIlroy WE, Mihailidis A. Reducing fall risk by improving balance control: Development, evaluation and knowledge-translation of new approaches. Journal of Safety Research. 2011;42: 473–485.

30. Finlayson ML, Peterson EW. Falls, aging, and disability. Physical Medicine and Rehabilitation Clinics of North America. 2010;21: 357–373.

31. Axer H, Axer M, Sauer H, Witte OW, Hagemann G. Falls and gait disorders in geriatric neurology. Clinical Neurology and Neurosurgery. 2010;112: 265–274.

32. Weinstein M, Booth J. Preventing falls in older adults: A multifactorial approach. Home Health Care Management and Practice. 2006;19: 45–50.

33. American Geriatrics Society. AGS/BGS clinical practice guideline: Prevention of falls in older persons. Available: http://www.americangeriatrics.org/health_care_professionals/clinical_practice/clinical_guidelines_recommendations/prevention_of_falls_summary_of_recommendations

34. Blake AJ, Morgan K, Bendall MJ, Dallosso H, Ebrahim SB, Arie TH, Fentem PH, Bassey EJ. Falls by elderly people at home: Prevalence and associated factors. Age and Ageing. 1988;17: 365–372.

35. Prudham D, Evans JG. Factors associated with falls in the elderly: A community study. Age and Ageing. 1981;10: 141–146.

36. Fleming J, Matthews FE, Brayne C. Falls in advanced old age: Recalled falls and prospective follow-up of over-90-year-olds in the Cambridge City over-75s cohort study. BMC Geriatrics. 2008;8(6).

37. Schoene D, Wu SM-S, Mikolaizak AS, Menant JC, Smith ST, Delbaere K, Lord SR. Discriminative ability and predictive validity of the Timed Up and Go Test in identifying older people who fall: Systematic review and meta-analysis. Journal of the American Geriatrics Society. 2013;61: 202–208.

38. Rivolta MW, Aktaruzzaman M, Rizzo G, Lafortuna CL, Ferrarin M, Bovi G, Bonardi DR, Sassi R. Automatic vs. Clinical assessment of fall risk in older individuals: A proof of

concept. 2015 37th Annual International Conference of the IEEE Engineering in Medicine and Biology Society (EMBC). IEEE; 2015. pp. 6935–6938.

39. Podsiadlo D, Richardson S. The timed "Up & Go": A test of basic functional mobility for frail elderly persons. Journal of the American Geriatrics Society. 1991;39: 142–148.

40. Shany T, Wang K, Liu Y, Lovell NH, Redmond SJ. Review: Are we stumbling in our quest to find the best predictor? Over-optimism in sensor-based models for predicting falls in older adults. Healthcare Technology Letters. 2015;2: 79–88.

41. Tinetti ME, Speechley M, Ginter SF. Risk factors for falls among elderly persons living in the community. New England Journal of Medicine. 1988;319: 1701–1707.

42. Yamada M, Higuchi T, Mori S, Uemura K, Nagai K, Aoyama T, Ichihashi N. Maladaptive turning and gaze behavior induces impaired stepping on multiple footfall targets during gait in older individuals who are at high risk of falling. Archives of Gerontology and Geriatrics. 2012;54: e102–e108.

43. Akram SB, Frank JS, Chenouri S. Turning behavior in healthy older adults: Is there a preference for step versus spin turns? Gait and Posture. 2010;31: 23–26.

44. Prieto TE, Myklebust JB, Hoffmann RG, Lovett EG, Myklebust BM. Measures of postural steadiness: Differences between healthy young and elderly adults. IEEE Transactions on Biomedical Engineering. 1996;43: 956–966.

45. Bellanca JL, Lowry KA, VanSwearingen JM, Brach JS, Redfern MS. Harmonic ratios: A quantification of step to step symmetry. Journal of Biomechanics. 2013;46: 828–831.

46. Doi T, Hirata S, Ono R, Tsutsumimoto K, Misu S, Ando H. The harmonic ratio of trunk acceleration predicts falling among older people: Results of a 1-year prospective study. Journal of Neuroengineering and Rehabilitation. 2013;10(7).

47. Yack HJ, Berger RC. Dynamic stability in the elderly: Identifying a possible measure. Journal of Gerontology. 1993;48: M225–M230.

48. Menz HB, Lord SR, Fitzpatrick RC. Acceleration patterns of the head and pelvis when walking are associated with risk of falling in community-dwelling older people. The Journals of Gerontology Series A: Biological Sciences and Medical Sciences. 2003;58: M446–M452.

49. Punt M, Bruijn SM, van Schooten KS, Pijnappels M, van de Port IG, Wittink H, van Dieën JH. Characteristics of daily life gait in fall and non fall-prone stroke survivors and controls. Journal of Neuroengineering and Rehabilitation. 2016;13(67).

50. Weiss A, Brozgol M, Dorfman M, Herman T, Shema S, Giladi N, Hausdorff JM. Does the evaluation of gait quality during daily life provide insight into fall risk? A novel approach using 3-day accelerometer recordings. Neurorehabilitation and Neural Repair. 2013;27: 742–752.

51. Rispens SM, van Schooten KS, Pijnappels M, Daffertshofer A, Beek PJ, van Dieën JH. Do extreme values of daily-life gait characteristics provide more information about fall risk than median values? JMIR Research Protocols. 2015;4: e4.

52. Friedman J, Hastie T, Tibshirani R. The elements of statistical learning. Springer, Berlin: Springer series in statistics; 2001.

53. Guyon I, Elisseeff A. An introduction to variable and feature selection. Journal of Machine Learning Research. 2003;3: 1157–1182.

54. Ding C, Peng H. Minimum redundancy feature selection from microarray gene expression data. Journal of Bioinformatics and Computational Biology. 2005;3: 185–205.

55. Pedregosa F, Varoquaux G, Gramfort A, Michel V, Thirion B, Grisel O, Blondel M, Prettenhofer P, Weiss R, Dubourg V, Vanderplas J. Scikit-learn: Machine learning in Python. Journal of Machine Learning Research. 2011;12: 2825–2830.

56. Guyon I, Weston J, Barnhill S, Vapnik V. Gene selection for cancer classification using support vector machines. Machine Learning. 2002;46: 389–422.

57. Wolpert DH. The supervised learning no-free-lunch theorems. Soft Computing and Industry. Springer; 2002. pp. 25–42.

58. Cortes C, Vapnik V. Support-vector networks. Machine Learning. 1995;20: 273–297.

59. James G, Witten D, Hastie T, Tibshirani R. An introduction to statistical learning. New York: Springer; 2013.

60. Jernigan ME, Fieguth PW. Pattern Recognition in a Nutshell. Waterloo, ON: University of Waterloo Publishing; 2012.

61. Alpaydin E. Introduction to machine learning. Cambridge, MA: MIT press; 2014.

62. Breiman L. Bagging predictors. Machine Learning. 1996;24: 123–140.

63. WHO | Falls. In: WHO. [cited 12 Feb 2017]. Available: http://www.who.int/mediacentre/factsheets/fs344/en/

64. Guide MU. The mathworks. Inc, Natick, MA. 1998;5: 333.

65. Smidt GL, Arora JS, Johnston RC. Accelerographic analysis of several types of walking. American Journal of Physical Medicine and Rehabilitation. 1971;50: 285–300.

66. Grus J. Data science from scratch: first principles with python. Sebastopol, CA: O'Reilly Media, Inc.; 2015.

67. Liang S, Ning Y, Li H, Wang L, Mei Z, Ma Y, Zhao G. Feature selection and predictors of falls with foot force sensors using kNN-based algorithms. Sensors. 2015;15: 29393–29407.

68. Shapiro SS, Wilk MB. An analysis of variance test for normality (complete samples). Biometrika. 1965;52: 591–611.

69. Wilcoxon F. Individual comparisons by ranking methods. Biometrics Bulletin. 1945;1: 80–83.

70. Mann HB, Whitney DR. On a test of whether one of two random variables is stochastically larger than the other. The Annals of Mathematical Statistics. 1947; 50–60.

71. Benjamini Y, Hochberg Y. Controlling the false discovery rate: A practical and powerful approach to multiple testing. Journal of the Royal Statistical Society Series B (Methodological). 1995; 289–300.

72. Shaffer JP. Multiple hypothesis testing. Annual Review of Psychology. 1995;46: 561-584.

73. Ihaka R, Gentleman R. R: A language for data analysis and graphics. Journal of Computational and Graphical Statistics. 1996;5: 299–314.

74. Boser BE, Guyon IM, Vapnik VN. A training algorithm for optimal margin classifiers. Proceedings of the Fifth Annual Workshop on Computational Learning Theory. ACM; 1992. pp. 144–152.

75. Matthews BW. Comparison of the predicted and observed secondary structure of T4 phage lysozyme. Biochimica et Biophysica Acta (BBA)-Protein Structure. 1975;405: 442–451.

76. van Rijsbergen CJ. A theoretical basis for the use of co-occurrence data in information retrieval. Journal of Documentation. 1977;33: 106–119.

77. Kendell C, Lemaire ED, Losier Y, Wilson A, Chan A, Hudgins B. A novel approach to surface electromyography: An exploratory study of electrode-pair selection based on signal characteristics. Journal of Neuroengineering and Rehabilitation. 2012; 9(24).

78. Hsu P-L, Robbins H. Complete convergence and the law of large numbers. Proceedings of the National Academy of Sciences. 1947;33: 25–31.

79. Latt MD, Menz HB, Fung VS, Lord SR. Acceleration patterns of the head and pelvis during gait in older people with Parkinson's disease: A comparison of fallers and nonfallers. The Journals of Gerontology Series A: Biological Sciences and Medical Sciences. 2009; glp009.

80. Shumway-Cook A, Brauer S, Woollacott M. Predicting the probability for falls in community-dwelling older adults using the Timed Up & Go Test. Physical Therapy. 2000;80: 896–903.

81. Maaten L van der, Hinton G. Visualizing data using t-SNE. Journal of Machine Learning Research. 2008;9: 2579–2605.

Appendix A:

Between Walking Condition Post-hoc Results

Table A.1. Means, standard deviations, and *p*-values between turn and straight walking conditions for faller and non-faller groups for temporal features. ST: Stride-time**,** Max: maximum, Min: minimum, SD: standard deviation, LB: lower back, $\bar{x}$: mean. Bold indicates a significant difference ($p < 0.05$).

Features	Fallers					Non-Fallers				
	Turn		Straight			Turn		Straight		
	$\bar{x}$	SD	$\bar{x}$	SD	*p*	$\bar{x}$	SD	$\bar{x}$	SD	*p*
Max ST LB	1.362	0.190	1.101	0.113	**0.000**	1.302	0.199	1.074	0.184	**0.000**
Max Cadence LB	127.91	23.70	116.55	11.76	**0.005**	126.70	16.91	122.57	11.26	0.055
Min ST LB	0.988	0.164	1.042	0.095	**0.030**	0.975	0.141	0.994	0.096	0.379
Min Cadence LB	95.57	12.23	110.89	11.67	**0.000**	98.59	13.20	115.00	12.79	**0.000**
Mean ST LB	1.138	0.146	1.069	0.101	**0.000**	1.109	0.144	1.025	0.113	**0.000**
Mean Cadence LB	111.10	15.17	113.72	11.78	0.095	112.68	13.23	118.93	11.30	**0.001**
SD ST LB	0.111	0.051	0.018	0.012	**0.000**	0.100	0.062	0.024	0.040	**0.000**
SD Cadence LB	9.365	5.586	1.722	0.765	**0.000**	8.422	4.496	2.232	1.825	**0.000**

Table A.2. Means, standard deviations, and *p*-values between turn and straight walking conditions for faller and non-faller groups for maximum of descriptive statistic features. Max: maximum, SD: standard deviation, Post: posterior direction, Ant: anterior direction, Sup: superior direction, Inf: inferior direction, RS: right shank, LS: left shank, LB: lower back, $\bar{x}$: mean. Bold indicates a significant difference ($p < 0.05$).

Feature	Fallers					Non-Fallers				
	Turn		Straight			Turn		Straight		
	$\bar{x}$	SD	$\bar{x}$	SD	*p*	$\bar{x}$	SD	$\bar{x}$	SD	*p*
Max Mean Left RS	0.350	0.141	0.309	0.178	0.066	0.365	0.098	0.317	0.129	**0.006**
Max SD Left RS	0.315	0.131	0.286	0.151	0.095	0.333	0.103	0.310	0.137	0.140
Max Max Left RS	1.087	0.412	0.900	0.416	0.002	1.152	0.374	0.966	0.380	**0.001**
Max Mean Right	0.346	0.146	0.205	0.084	**0.000**	0.409	0.158	0.230	0.075	**0.000**
Max SD Right RS	0.286	0.117	0.185	0.081	**0.000**	0.310	0.107	0.210	0.080	**0.000**
Max Max Right RS	1.026	0.403	0.693	0.296	**0.000**	1.123	0.347	0.767	0.297	**0.000**
Max Mean Post RS	0.385	0.117	0.334	0.086	**0.001**	0.417	0.130	0.362	0.099	**0.000**
Max SD Post RS	0.353	0.102	0.354	0.105	0.959	0.385	0.123	0.347	0.093	**0.005**
Max Mean Ant RS	0.479	0.179	0.518	0.179	0.081	0.579	0.237	0.667	0.282	**0.000**
Max SD Ant RS	0.545	0.223	0.579	0.168	0.060	0.657	0.237	0.740	0.288	**0.001**
Max Mean Inf RS	0.324	0.117	0.263	0.124	**0.000**	0.362	0.113	0.283	0.099	**0.000**
Max SD Inf RS	0.305	0.109	0.251	0.122	**0.001**	0.336	0.104	0.278	0.108	**0.000**
Max Max Inf RS	1.136	0.410	0.914	0.410	**0.000**	1.214	0.377	1.011	0.368	**0.000**
Max Mean Sup RS	0.321	0.148	0.178	0.066	**0.000**	0.354	0.129	0.205	0.072	**0.000**
Max SD Sup RS	0.289	0.118	0.155	0.055	**0.000**	0.314	0.113	0.178	0.072	**0.000**
Max Max Sup RS	0.994	0.352	0.578	0.202	**0.000**	1.081	0.342	0.652	0.240	**0.000**

Max Mean Left LS	0.411	0.169	0.265	0.087	**0.000**	0.443	0.161	0.301	0.126	**0.000**
Max SD Left LS	0.381	0.168	0.275	0.113	**0.000**	0.403	0.157	0.302	0.153	**0.000**
Max Max Left LS	1.314	0.575	1.022	0.414	**0.000**	1.422	0.539	1.098	0.466	**0.000**
Max Mean Rght LS	0.334	0.097	0.216	0.056	**0.000**	0.372	0.095	0.238	0.066	**0.000**
Max SD Right LS	0.291	0.082	0.246	0.096	**0.020**	0.328	0.084	0.246	0.062	**0.000**
Max Max Right LS	0.994	0.286	0.859	0.324	**0.041**	1.076	0.264	0.840	0.224	**0.000**
Max Mean Ant LS	0.412	0.201	0.535	0.207	**0.000**	0.514	0.208	0.644	0.228	**0.000**
Max SD Ant LS	0.456	0.221	0.596	0.208	**0.000**	0.552	0.197	0.688	0.212	**0.000**
Max Max Ant LS	1.676	0.717	1.944	0.601	**0.004**	1.897	0.608	2.184	0.593	**0.000**
Max Mean Inf LS	0.329	0.114	0.246	0.068	**0.000**	0.358	0.118	0.280	0.086	**0.000**
Max SD Inf LS	0.343	0.123	0.266	0.083	**0.000**	0.378	0.129	0.292	0.111	**0.000**
Max Max Inf LS	1.315	0.473	1.046	0.326	**0.000**	1.427	0.492	1.099	0.415	**0.000**
Max Mean Sup LS	0.356	0.178	0.236	0.075	**0.000**	0.408	0.138	0.260	0.124	**0.000**
Max SD Sup LS	0.368	0.181	0.262	0.127	**0.000**	0.375	0.140	0.260	0.143	**0.000**
Max Max Sup LS	1.270	0.561	0.948	0.452	**0.000**	1.325	0.474	0.929	0.448	**0.000**
Max Mean Left LB	0.202	0.091	0.176	0.078	**0.002**	0.240	0.100	0.201	0.079	**0.008**
Max SD Left LB	0.165	0.091	0.140	0.046	0.171	0.193	0.105	0.164	0.074	**0.034**
Max Max Left LB	0.636	0.317	0.537	0.170	0.081	0.747	0.374	0.613	0.262	**0.003**
Max Mean Rght LB	0.221	0.091	0.172	0.085	**0.001**	0.225	0.063	0.182	0.080	**0.000**
Max SD Right LB	0.177	0.091	0.143	0.062	**0.030**	0.185	0.056	0.146	0.061	**0.000**
Max Max Right LB	0.615	0.301	0.524	0.221	0.056	0.636	0.198	0.521	0.206	**0.000**
Max Mean Post LB	0.209	0.084	0.175	0.079	**0.009**	0.225	0.092	0.178	0.086	**0.002**
Max SD Post LB	0.168	0.067	0.117	0.038	**0.000**	0.174	0.071	0.123	0.057	**0.000**
Max Max Post LB	0.618	0.257	0.451	0.159	**0.001**	0.621	0.268	0.448	0.197	**0.000**
Max Mean Ant LB	0.243	0.131	0.218	0.104	0.138	0.315	0.172	0.277	0.120	0.267
Max SD Ant LB	0.243	0.153	0.185	0.074	**0.040**	0.296	0.176	0.244	0.118	**0.031**
Max Max Ant LB	0.864	0.465	0.628	0.224	**0.002**	1.001	0.527	0.794	0.340	**0.004**
Max SD Inf LB	0.182	0.087	0.161	0.054	0.186	0.208	0.089	0.179	0.071	**0.004**
Max Max Inf LB	0.692	0.329	0.602	0.205	0.109	0.786	0.354	0.643	0.245	**0.001**
Max Mean Sup LB	0.217	0.078	0.136	0.059	**0.000**	0.232	0.089	0.159	0.067	**0.000**
Max SD Sup LB	0.175	0.088	0.106	0.036	**0.000**	0.178	0.081	0.124	0.062	**0.000**
Max Max Sup LB	0.648	0.299	0.419	0.135	**0.000**	0.678	0.314	0.469	0.228	**0.000**

Table A.3. Means, standard deviations, and *p*-values between turn and straight walking conditions for faller and non-faller groups for minimum of descriptive statistic features. Max: maximum, Min: minimum, SD: standard deviation, Post: posterior direction, Ant: anterior direction, Sup: superior direction, Inf: inferior direction, RS: right shank, LS: left shank, LB: lower back, $\bar{x}$: mean. Bold indicates a significant difference ($p < 0.05$).

Feature	Fallers					Non-Fallers				
	Turn		Straight			Turn		Straight		
	$\bar{x}$	SD	$\bar{x}$	SD	*p*	$\bar{x}$	SD	$\bar{x}$	SD	*p*
Min Mean Left RS	0.155	0.076	0.246	0.136	**0.000**	0.153	0.056	0.250	0.098	**0.000**
Min SD Left RS	0.130	0.066	0.234	0.139	**0.000**	0.125	0.041	0.246	0.116	**0.000**
Min Max Left RS	0.466	0.195	0.751	0.392	**0.000**	0.460	0.141	0.793	0.325	**0.000**
Min Mean Right RS	0.141	0.073	0.171	0.070	**0.000**	0.160	0.058	0.190	0.062	**0.000**
Min SD Right RS	0.103	0.050	0.153	0.076	**0.000**	0.122	0.045	0.171	0.068	**0.000**
Min Max Right RS	0.424	0.186	0.576	0.275	**0.000**	0.476	0.169	0.622	0.242	**0.000**
Min Mean Post RS	0.199	0.078	0.279	0.074	**0.000**	0.200	0.069	0.309	0.079	**0.000**
Min SD Post RS	0.169	0.069	0.289	0.088	**0.000**	0.175	0.054	0.291	0.076	**0.000**
Min Max Post RS	0.584	0.237	1.029	0.341	**0.000**	0.620	0.194	1.057	0.284	**0.000**
Min Mean Ant RS	0.238	0.081	0.423	0.126	**0.000**	0.269	0.109	0.532	0.212	**0.000**
Min SD Ant RS	0.190	0.082	0.483	0.146	**0.000**	0.237	0.125	0.611	0.243	**0.000**
Min Max Ant RS	0.752	0.269	1.706	0.488	**0.000**	0.899	0.413	2.006	0.697	**0.000**
Min Mean Inf RS	0.178	0.088	0.226	0.107	**0.000**	0.187	0.058	0.236	0.081	**0.000**
Min SD Inf RS	0.143	0.075	0.214	0.115	**0.000**	0.154	0.045	0.231	0.093	**0.000**
Min Max Inf RS	0.529	0.244	0.773	0.381	**0.000**	0.569	0.160	0.836	0.312	**0.000**
Min Mean Sup RS	0.134	0.053	0.142	0.046	0.144	0.149	0.053	0.164	0.055	**0.045**
Min SD Sup RS	0.098	0.033	0.116	0.039	**0.008**	0.110	0.037	0.136	0.056	**0.000**
Min Max Sup RS	0.373	0.103	0.432	0.146	**0.032**	0.420	0.119	0.492	0.183	**0.002**
Min Mean Left LS	0.175	0.064	0.225	0.077	**0.000**	0.187	0.064	0.248	0.103	**0.000**
Min SD Left LS	0.120	0.049	0.226	0.098	**0.000**	0.128	0.054	0.239	0.126	**0.000**
Min Max Left LS	0.511	0.184	0.855	0.367	**0.000**	0.538	0.196	0.881	0.385	**0.000**
Min Mean Right LS	0.147	0.043	0.177	0.046	**0.003**	0.147	0.047	0.188	0.046	**0.000**
Min SD Right LS	0.131	0.035	0.194	0.082	**0.000**	0.133	0.035	0.186	0.044	**0.000**
Min Max Right LS	0.462	0.126	0.683	0.287	**0.000**	0.473	0.133	0.634	0.175	**0.000**
Min Mean Post LS	0.190	0.096	0.272	0.096	**0.000**	0.200	0.081	0.296	0.098	**0.000**
Min SD Post LS	0.182	0.082	0.256	0.088	**0.000**	0.177	0.069	0.264	0.093	**0.000**
Min Max Post LS	0.627	0.275	0.916	0.313	**0.000**	0.631	0.252	0.946	0.338	**0.000**
Min Mean Ant LS	0.248	0.115	0.444	0.159	**0.000**	0.258	0.118	0.528	0.193	**0.000**
Min SD Ant LS	0.238	0.121	0.512	0.184	**0.000**	0.248	0.125	0.586	0.189	**0.000**
Min Max Ant LS	0.852	0.376	1.704	0.552	**0.000**	0.874	0.389	1.890	0.542	**0.000**
Min Mean Inf LS	0.185	0.041	0.212	0.060	**0.009**	0.195	0.064	0.234	0.072	**0.000**
Min SD Inf LS	0.144	0.038	0.221	0.076	**0.000**	0.156	0.055	0.235	0.098	**0.000**
Min Max Inf LS	0.557	0.125	0.862	0.286	**0.000**	0.594	0.185	0.879	0.360	**0.000**
Min SD Sup LS	0.129	0.054	0.211	0.109	**0.000**	0.139	0.050	0.198	0.111	**0.000**
Min Max Sup LS	0.510	0.184	0.770	0.394	**0.000**	0.545	0.175	0.716	0.351	**0.000**
Min Mean Left LB	0.120	0.051	0.139	0.055	**0.034**	0.139	0.056	0.153	0.059	**0.026**
Min SD Left LB	0.087	0.043	0.109	0.038	**0.006**	0.101	0.048	0.121	0.048	**0.007**
Min Max Left LB	0.333	0.166	0.409	0.137	**0.006**	0.382	0.187	0.452	0.184	**0.012**

Min SD Right LB	0.090	0.039	0.115	0.055	**0.010**	0.099	0.053	0.110	0.053	0.192
Min Max Right LB	0.317	0.126	0.420	0.192	**0.004**	0.342	0.190	0.387	0.191	0.161
Min Mean Ant LB	0.137	0.073	0.169	0.079	0.090	0.172	0.103	0.201	0.080	0.095
Min Mean Inf LB	0.131	0.043	0.177	0.072	**0.000**	0.149	0.050	0.179	0.074	**0.002**
Min SD Inf LB	0.102	0.035	0.131	0.047	**0.000**	0.116	0.050	0.137	0.054	**0.015**
Min Max Inf LB	0.385	0.144	0.489	0.180	**0.000**	0.429	0.183	0.498	0.187	**0.030**

Table A.4. Means, standard deviations, and *p*-values between turn and straight walking conditions for faller and non-faller groups for mean descriptive statistic features. Max: maximum, SD: standard deviation, Post: posterior direction, Ant: anterior direction, Sup: superior direction, Inf: inferior direction, RS: right shank, LS: left shank, LB: lower back, $\bar{x}$: mean. Bold indicates a significant difference ($p < 0.05$).

Feature	Fallers					Non-Fallers				
	Turn		Straight			Turn		Straight		
	$\bar{x}$	SD	$\bar{x}$	SD	*p*	$\bar{x}$	SD	$\bar{x}$	SD	*p*
Mean Mean Left RS	0.242	0.106	0.277	0.158	0.077	0.244	0.067	0.283	0.111	**0.014**
Mean SD Left RS	0.217	0.096	0.261	0.146	**0.023**	0.213	0.062	0.277	0.125	**0.000**
Mean Max Left RS	0.749	0.289	0.828	0.407	0.157	0.754	0.205	0.874	0.346	**0.005**
Mean mean R RS	0.233	0.106	0.188	0.078	**0.000**	0.256	0.088	0.208	0.067	**0.000**
Mean SD Right RS	0.183	0.079	0.169	0.080	**0.043**	0.203	0.066	0.189	0.073	0.070
Mean Max Rght RS	0.693	0.276	0.636	0.290	**0.016**	0.752	0.224	0.692	0.268	**0.024**
Mean mean Post RS	0.284	0.089	0.304	0.080	**0.016**	0.302	0.090	0.334	0.089	**0.000**
Mean SD Post RS	0.254	0.073	0.321	0.096	**0.000**	0.270	0.076	0.318	0.084	**0.000**
Mean Max Post RS	0.878	0.260	1.167	0.392	**0.000**	0.960	0.287	1.199	0.353	**0.000**
Mean Mean Ant RS	0.348	0.123	0.464	0.136	**0.000**	0.410	0.163	0.596	0.248	**0.000**
Mean SD Ant RS	0.344	0.130	0.531	0.157	**0.000**	0.431	0.182	0.676	0.265	**0.000**
Mean Max Ant RS	1.296	0.444	1.851	0.527	**0.000**	1.536	0.570	2.193	0.742	**0.000**
Mean SD Inf RS	0.219	0.086	0.234	0.119	0.316	0.232	0.067	0.254	0.100	0.085
Mean Mean Sup RS	0.216	0.093	0.160	0.057	**0.000**	0.235	0.074	0.183	0.062	**0.000**
Mean SD Sup RS	0.182	0.073	0.135	0.049	**0.000**	0.193	0.058	0.156	0.063	**0.000**
Mean Max Sup RS	0.654	0.218	0.502	0.177	**0.000**	0.697	0.177	0.570	0.211	**0.000**
Mean Mean Left LS	0.272	0.107	0.244	0.083	0.090	0.294	0.101	0.272	0.114	**0.006**
Mean SD Left LS	0.230	0.100	0.252	0.107	**0.040**	0.247	0.096	0.270	0.137	0.237
Mean Max Left LS	0.860	0.348	0.943	0.393	0.060	0.923	0.331	0.988	0.420	0.562
Mean Mean R LS	0.231	0.061	0.196	0.051	**0.004**	0.249	0.057	0.212	0.054	**0.000**
Mean Mean Post LS	0.256	0.106	0.295	0.102	**0.000**	0.282	0.106	0.327	0.110	**0.000**
Mean SD Post LS	0.237	0.086	0.278	0.089	**0.000**	0.251	0.084	0.293	0.102	**0.000**
Mean Max Post LS	0.830	0.284	1.004	0.327	**0.000**	0.907	0.291	1.070	0.379	**0.000**
Mean Mean Ant LS	0.330	0.158	0.493	0.188	**0.000**	0.374	0.162	0.584	0.210	**0.000**
Mean SD Ant LS	0.344	0.173	0.559	0.201	**0.000**	0.384	0.164	0.638	0.202	**0.000**
Mean Max Ant LS	1.238	0.525	1.837	0.586	**0.000**	1.330	0.501	2.045	0.573	**0.000**
Mean Mean Inf LS	0.251	0.074	0.229	0.063	0.126	0.271	0.081	0.256	0.079	0.062
Mean Mean Sup LS	0.261	0.107	0.215	0.070	**0.011**	0.285	0.091	0.231	0.107	**0.000**
Mean SD Post LB	0.127	0.054	0.107	0.034	0.054	0.125	0.055	0.108	0.051	0.060
Mean Max Post LB	0.458	0.189	0.408	0.142	0.152	0.456	0.208	0.396	0.183	0.075
Mean Mean Inf LB	0.167	0.064	0.196	0.085	**0.002**	0.190	0.060	0.207	0.085	0.071
Mean Mean Sup LB	0.168	0.062	0.123	0.053	**0.000**	0.173	0.058	0.144	0.061	**0.012**
Mean SD Sup LB	0.126	0.061	0.094	0.033	**0.002**	0.128	0.049	0.111	0.056	0.069
Mean Max Sup LB	0.470	0.204	0.362	0.116	**0.002**	0.485	0.197	0.414	0.199	0.063

Table A.5. Means, standard deviations, and *p*-values between turn and straight walking conditions for faller and non-faller groups for standard deviation of descriptive statistic features. Max: maximum, SD: standard deviation, Post: posterior direction, Ant: anterior direction, Sup: superior direction, Inf: inferior direction, RS: right shank, LS: left shank, LB: lower back, $\bar{x}$: mean. Bold indicates a significant difference ($p < 0.05$).

Feature	Fallers					Non-Fallers				
	Turn		Straight			Turn		Straight		
	$\bar{x}$	SD	$\bar{x}$	SD	*p*	$\bar{x}$	SD	$\bar{x}$	SD	*p*
SD Mean Left RS	0.057	0.023	0.018	0.015	**0.000**	0.062	0.019	0.019	0.011	**0.000**
SD SD Left RS	0.056	0.024	0.016	0.007	**0.000**	0.061	0.021	0.018	0.009	**0.000**
SD Max Left RS	0.181	0.073	0.045	0.018	**0.000**	0.199	0.074	0.049	0.022	**0.000**
SD Mean Right RS	0.065	0.029	0.010	0.007	**0.000**	0.075	0.037	0.011	0.005	**0.000**
SD SD Right RS	0.057	0.026	0.009	0.006	**0.000**	0.057	0.021	0.011	0.005	**0.000**
SD Max Right RS	0.185	0.083	0.035	0.016	**0.000**	0.186	0.071	0.041	0.019	**0.000**
SD Mean Post RS	0.056	0.027	0.016	0.013	**0.000**	0.062	0.026	0.015	0.006	**0.000**
SD SD Post RS	0.057	0.026	0.019	0.011	**0.000**	0.062	0.028	0.016	0.007	**0.000**
SD Max Post RS	0.193	0.089	0.079	0.046	**0.000**	0.215	0.096	0.081	0.043	**0.000**
SD Mean Ant RS	0.073	0.038	0.030	0.045	**0.000**	0.090	0.037	0.038	0.023	**0.000**
SD SD Ant RS	0.106	0.050	0.029	0.019	**0.000**	0.126	0.044	0.037	0.019	**0.000**
SD Max Ant RS	0.381	0.200	0.084	0.035	**0.000**	0.416	0.148	0.102	0.048	**0.000**
SD Mean Inf RS	0.043	0.011	0.011	0.008	**0.000**	0.051	0.019	0.013	0.007	**0.000**
SD SD Inf RS	0.049	0.017	0.011	0.004	**0.000**	0.052	0.019	0.013	0.006	**0.000**
SD Max Inf RS	0.178	0.061	0.042	0.018	**0.000**	0.186	0.068	0.050	0.024	**0.000**
SD Mean Sup RS	0.057	0.030	0.011	0.007	**0.000**	0.060	0.029	0.012	0.006	**0.000**
SD SD Sup RS	0.059	0.028	0.012	0.007	**0.000**	0.060	0.027	0.012	0.007	**0.000**
SD Max Sup RS	0.188	0.082	0.044	0.023	**0.000**	0.193	0.078	0.045	0.022	**0.000**
SD Mean Left LS	0.078	0.041	0.012	0.005	**0.000**	0.081	0.040	0.015	0.009	**0.000**
SD SD Left LS	0.087	0.044	0.014	0.006	**0.000**	0.089	0.040	0.017	0.010	**0.000**
SD Max Left LS	0.259	0.150	0.050	0.023	**0.000**	0.274	0.128	0.058	0.030	**0.000**
SD Mean Right LS	0.057	0.024	0.012	0.005	**0.000**	0.066	0.021	0.014	0.008	**0.000**
SD SD Right LS	0.047	0.017	0.015	0.008	**0.000**	0.057	0.021	0.017	0.009	**0.000**
SD Max Right LS	0.155	0.055	0.050	0.027	**0.000**	0.175	0.059	0.059	0.024	**0.000**
SD Mean Post LS	0.041	0.017	0.013	0.005	**0.000**	0.049	0.023	0.018	0.008	**0.000**
SD SD Post LS	0.037	0.015	0.013	0.004	**0.000**	0.045	0.022	0.016	0.006	**0.000**
SD Max Post LS	0.140	0.044	0.055	0.018	**0.000**	0.172	0.067	0.071	0.030	**0.000**
SD Mean Ant LS	0.049	0.030	0.028	0.020	**0.000**	0.075	0.032	0.033	0.016	**0.000**
SD SD Ant LS	0.063	0.032	0.025	0.011	**0.000**	0.091	0.031	0.029	0.011	**0.000**
SD Max Ant LS	0.241	0.116	0.070	0.026	**0.000**	0.302	0.101	0.084	0.031	**0.000**
SD Mean Inf LS	0.043	0.021	0.010	0.004	**0.000**	0.048	0.019	0.013	0.007	**0.000**
SD SD Inf LS	0.062	0.031	0.013	0.005	**0.000**	0.068	0.027	0.016	0.007	**0.000**
SD Max Inf LS	0.231	0.121	0.054	0.025	**0.000**	0.251	0.104	0.061	0.029	**0.000**
SD Mean Sup LS	0.050	0.034	0.012	0.005	**0.000**	0.064	0.028	0.014	0.009	**0.000**
SD SD Sup LS	0.075	0.045	0.016	0.008	**0.000**	0.075	0.035	0.017	0.011	**0.000**
SD Max Sup LS	0.229	0.136	0.054	0.026	**0.000**	0.240	0.109	0.059	0.034	**0.000**
SD Mean Left LB	0.025	0.015	0.011	0.007	**0.000**	0.030	0.025	0.014	0.007	**0.000**
SD SD Left LB	0.025	0.023	0.009	0.004	**0.000**	0.028	0.030	0.013	0.009	**0.000**

SD Max Left LB	0.096	0.085	0.038	0.017	**0.000**	0.110	0.105	0.048	0.031	**0.000**
SD Mean Right LB	0.032	0.026	0.010	0.006	**0.000**	0.031	0.021	0.012	0.006	**0.000**
SD SD Right LB	0.028	0.022	0.009	0.004	**0.000**	0.027	0.018	0.010	0.005	**0.000**
SD Max Right LB	0.095	0.068	0.032	0.014	**0.000**	0.091	0.051	0.039	0.019	**0.000**
SD Mean Post LB	0.026	0.021	0.010	0.008	**0.000**	0.029	0.022	0.010	0.006	**0.000**
SD SD Post LB	0.024	0.021	0.006	0.004	**0.000**	0.025	0.021	0.009	0.006	**0.000**
SD Max Post LB	0.093	0.077	0.027	0.018	**0.000**	0.089	0.076	0.032	0.020	**0.000**
SD Mean Ant LB	0.032	0.027	0.014	0.009	**0.000**	0.043	0.041	0.022	0.016	**0.001**
SD SD Ant LB	0.038	0.035	0.014	0.006	**0.001**	0.043	0.040	0.021	0.018	**0.001**
SD Max Ant LB	0.136	0.113	0.046	0.020	**0.000**	0.146	0.120	0.064	0.054	**0.000**
SD Mean Inf LB	0.023	0.013	0.011	0.008	**0.000**	0.029	0.016	0.015	0.008	**0.000**
SD SD Inf LB	0.025	0.018	0.009	0.004	**0.000**	0.029	0.025	0.012	0.006	**0.000**
SD Max Inf LB	0.098	0.075	0.035	0.015	**0.000**	0.109	0.100	0.043	0.022	**0.000**
SD Mean Sup LB	0.030	0.018	0.008	0.005	**0.000**	0.028	0.021	0.010	0.007	**0.000**
SD SD Sup LB	0.030	0.028	0.007	0.004	**0.000**	0.024	0.022	0.009	0.009	**0.000**
SD Max Sup LB	0.107	0.101	0.032	0.018	**0.000**	0.092	0.090	0.033	0.030	**0.000**

Table A.6. Means, standard deviations, and *p*-values between turn and straight walking conditions for faller and non-faller groups for first quartile fast Fourier transform features. Max: maximum, SD: standard deviation, AP: anterior-posterior axis, ML: medial-lateral axis, V: inferior-superior/vertical axis, RS: right shank, LS: left shank, LB: lower back, $\bar{x}$: mean. Bold indicates a significant difference ($p < 0.05$).

Feature	Fallers					Non-Fallers				
	Turn		Straight			Turn		Straight		
	$\bar{x}$	SD	$\bar{x}$	SD	*p*	$\bar{x}$	SD	$\bar{x}$	SD	*p*
Max FQFFT AP RS	71.06	13.35	14.38	6.68	**0.000**	78.05	11.52	15.60	8.59	**0.000**
Max FQFFT ML RS	71.22	10.88	15.41	6.36	**0.000**	77.22	9.84	16.40	8.83	**0.000**
Max FQFFT V RS	74.59	9.72	13.59	8.92	**0.000**	80.02	7.87	14.64	10.18	**0.000**
Max FQFFT AP LS	69.73	12.94	16.34	7.35	**0.000**	77.03	9.65	17.07	8.90	**0.000**
Max FQFFT ML LS	73.94	10.91	11.63	5.57	**0.000**	79.22	9.36	13.18	7.86	**0.000**
Max FQFFT V LS	75.54	9.31	13.04	8.87	**0.000**	80.90	7.37	14.68	11.26	**0.000**
Max FQFFT AP LB	75.51	10.50	14.35	8.46	**0.000**	81.63	6.73	14.25	7.55	**0.000**
Max FQFFT ML LB	75.92	12.43	12.09	5.91	**0.000**	84.00	8.95	13.94	8.68	**0.000**
Max FQFFT V LB	75.69	11.71	10.79	11.69	**0.000**	81.82	9.95	11.60	12.82	**0.000**
Min FQFFT AP RS	47.62	5.60	8.50	3.92	**0.000**	48.05	4.52	9.41	5.17	**0.000**
Min FQFFT ML RS	45.27	6.84	8.97	4.85	**0.000**	45.42	6.21	10.03	5.80	**0.000**
Min FQFFT V RS	51.40	6.59	7.69	3.05	**0.000**	49.69	6.88	8.51	4.09	**0.000**
Min FQFFT AP LS	44.49	5.36	9.46	4.87	**0.000**	46.79	4.71	10.32	5.94	**0.000**
Min FQFFT ML LS	49.23	6.20	7.00	2.97	**0.000**	49.67	5.96	8.02	4.29	**0.000**
Min FQFFT V LS	52.41	7.71	7.66	3.10	**0.000**	51.96	7.08	8.05	3.82	**0.000**
Min FQFFT AP LB	54.64	7.49	7.23	3.57	**0.000**	55.57	6.36	7.08	3.53	**0.000**
Min FQFFT ML LB	52.35	7.45	6.05	3.04	**0.000**	51.56	7.82	6.73	3.44	**0.000**
Min FQFFT V LB	52.99	5.84	3.55	2.02	**0.000**	51.55	6.62	3.91	3.87	**0.000**
Mean FQFFT AP RS	58.84	9.02	11.39	5.01	**0.000**	61.90	7.89	12.07	5.75	**0.000**
Mean FQFFT ML RS	58.43	8.24	12.43	5.68	**0.000**	60.59	8.08	12.68	5.99	**0.000**
Mean FQFFT V RS	63.91	7.68	10.47	5.60	**0.000**	64.28	7.15	11.15	6.12	**0.000**
Mean FQFFT AP LS	57.35	8.59	12.78	5.59	**0.000**	60.16	8.08	13.18	6.35	**0.000**
Mean FQFFT ML LS	61.69	8.16	9.27	4.06	**0.000**	64.04	7.29	10.25	4.98	**0.000**
Mean FQFFT V LS	64.79	7.22	10.27	5.88	**0.000**	65.52	7.31	10.94	6.39	**0.000**
Mean FQFFT AP LB	65.32	7.64	10.76	5.16	**0.000**	67.17	5.68	9.90	3.95	**0.000**
Mean FQFFT ML LB	64.00	9.35	8.84	3.50	**0.000**	66.46	7.83	9.72	4.70	**0.000**
Mean FQFFT V LB	64.40	7.62	6.99	6.07	**0.000**	64.88	8.33	7.10	6.58	**0.000**
SD FQFFT AP RS	7.24	4.62	1.82	1.58	**0.000**	9.60	4.31	1.88	1.82	**0.000**
SD FQFFT ML RS	8.24	3.90	1.96	1.65	**0.000**	9.48	3.15	2.01	1.96	**0.000**
SD FQFFT V RS	7.11	3.36	1.96	2.84	**0.000**	9.39	3.72	2.08	3.05	**0.000**
SD FQFFT AP LS	7.87	4.73	2.09	1.78	**0.000**	9.85	4.31	2.06	1.81	**0.000**
SD FQFFT ML LS	7.87	3.96	1.42	1.31	**0.000**	9.29	3.75	1.53	1.51	**0.000**
SD FQFFT V LS	7.35	3.86	1.84	2.77	**0.000**	9.19	4.10	2.26	3.46	**0.000**
SD FQFFT AP LB	6.48	3.90	2.22	2.27	**0.000**	8.24	3.60	2.20	2.15	**0.000**
SD FQFFT ML LB	7.55	4.89	1.83	1.54	**0.000**	10.27	4.78	2.12	2.01	**0.000**
SD FQFFT V LB	7.31	4.83	2.51	4.41	**0.001**	9.87	4.80	2.75	4.69	**0.000**

Table A.7. Means, standard deviations, and *p*-values between turn and straight walking conditions for faller and non-faller groups for ratio of even to odd harmonics features. Max: maximum, SD: standard deviation, AP: anterior-posterior axis, ML: medial-lateral axis, V: inferior-superior/vertical axis, RS: right shank, LS: left shank, LB: lower back, $\bar{x}$: mean. Bold indicates a significant difference ($p < 0.05$).

Feature	Fallers					Non-Fallers				
	Turn		Straight			Turn		Straight		
	$\bar{x}$	SD	$\bar{x}$	SD	*p*	$\bar{x}$	SD	$\bar{x}$	SD	*p*
Max REOH AP RS	1.332	0.237	1.728	0.762	**0.028**	1.312	0.217	1.551	0.403	**0.000**
Max REOH ML RS	1.325	0.214	1.538	0.386	**0.016**	1.295	0.184	1.545	0.418	**0.000**
Max REOH V RS	1.462	0.241	2.407	1.229	**0.000**	1.441	0.222	2.076	0.528	**0.000**
Max REOH AP LS	1.319	0.202	1.590	0.632	0.063	1.326	0.267	1.554	0.500	**0.004**
Max REOH ML LS	1.222	0.169	1.504	0.519	**0.003**	1.251	0.167	1.383	0.427	0.347
Max REOH V LS	1.430	0.317	2.300	0.890	**0.000**	1.418	0.214	2.096	0.679	**0.000**
Max REOH AP LB	1.907	0.538	4.575	1.685	**0.000**	2.122	0.663	5.240	2.000	**0.000**
Max REOH ML LB	1.334	0.226	0.964	0.289	**0.000**	1.320	0.279	0.957	0.314	**0.000**
Max REOH V LB	1.800	0.363	4.827	1.931	**0.000**	1.928	0.517	4.961	1.782	**0.000**
Min REOH AP RS	0.710	0.104	0.600	0.122	**0.002**	0.627	0.078	0.570	0.165	**0.025**
Min REOH ML RS	0.663	0.096	0.579	0.133	**0.012**	0.642	0.080	0.548	0.135	**0.000**
Min REOH AP LS	0.692	0.111	0.569	0.129	**0.001**	0.648	0.108	0.543	0.129	**0.000**
Min REOH AP LB	0.626	0.112	1.391	0.402	**0.000**	0.678	0.154	1.485	0.649	**0.000**
Min REOH ML LB	0.523	0.113	0.325	0.108	**0.000**	0.522	0.101	0.288	0.118	**0.000**
Min REOH V LB	0.697	0.078	1.339	0.459	**0.000**	0.706	0.141	1.426	0.708	**0.000**
Mean REOH V RS	1.011	0.097	1.284	0.205	**0.000**	0.974	0.062	1.243	0.180	**0.000**
Mean REOH ML LS	0.903	0.059	0.973	0.123	**0.008**	0.904	0.057	0.935	0.138	0.207
Mean REOH V LS	0.998	0.084	1.271	0.193	**0.000**	0.983	0.076	1.242	0.213	**0.000**
Mean REOH AP LB	1.147	0.207	2.645	0.704	**0.000**	1.263	0.293	3.066	0.995	**0.000**
Mean REOH ML LB	0.860	0.110	0.562	0.139	**0.000**	0.856	0.112	0.524	0.164	**0.000**
Mean REOH V LB	1.150	0.158	2.702	0.692	**0.000**	1.225	0.250	2.892	1.049	**0.000**
SD REOH AP RS	0.182	0.073	0.307	0.191	**0.001**	0.193	0.060	0.271	0.105	**0.000**
SD REOH ML RS	0.191	0.067	0.272	0.105	**0.003**	0.184	0.050	0.288	0.112	**0.000**
SD REOH V RS	0.228	0.069	0.470	0.304	**0.000**	0.218	0.060	0.390	0.130	**0.000**
SD REOH AP LS	0.186	0.062	0.284	0.156	**0.001**	0.193	0.067	0.280	0.130	**0.000**
SD REOH ML LS	0.162	0.048	0.233	0.139	**0.020**	0.176	0.046	0.213	0.107	**0**.288
SD REOH V LS	0.215	0.081	0.441	0.221	**0.000**	0.210	0.063	0.379	0.168	**0.000**
SD REOH AP LB	0.385	0.151	0.906	0.378	**0.000**	0.408	0.173	1.078	0.388	**0.000**
SD REOH ML LB	0.242	0.066	0.190	0.073	**0.010**	0.225	0.063	0.186	0.071	**0.008**
SD REOH V LB	0.326	0.098	1.013	0.413	**0.000**	0.353	0.142	1.014	0.401	**0.000**